

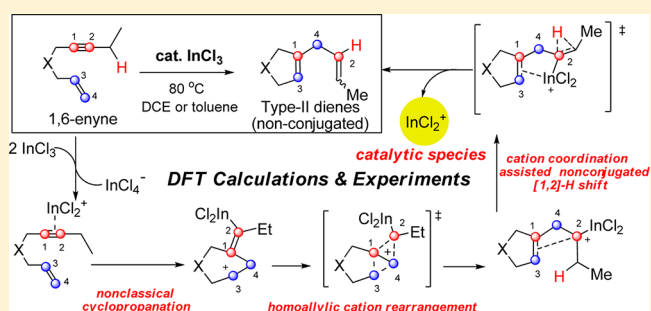
# DFT and Experimental Exploration of the Mechanism of $\text{InCl}_3$ -Catalyzed Type II Cycloisomerization of 1,6-Enynes: Identifying $\text{InCl}_2^+$ as the Catalytic Species and Answering Why Nonconjugated Dienes Are Generated

Lian-Gang Zhuo,<sup>†</sup> Ji-Ji Zhang,<sup>†</sup> and Zhi-Xiang Yu\*<sup>†</sup>

Beijing National Laboratory for Molecular Sciences (BNLMS), Key Laboratory of Bioorganic Chemistry and Molecular Engineering of Ministry of Education, College of Chemistry, Peking University, Beijing 100871, People's Republic of China

## Supporting Information

**ABSTRACT:**  $\text{InCl}_3$  and other In(III) species have been widely applied as catalysts in many reactions. However, what are the real catalytic species of these reactions? Through DFT calculations and experimental investigation of the mechanism and regioselectivity of  $\text{InCl}_3$ -catalyzed cycloisomerization reactions of 1,6-enynes (here all discussed 1,6-enynes are ene-internal-alkyne molecules), we propose that the catalytic species of this reaction is the in situ generated  $\text{InCl}_2^+$ . Further electrospray ionization high-resolution mass spectroscopy (ESI-HRMS) supported the existence of  $\text{InCl}_2^+$  in acetonitrile solution. This finding of  $\text{InCl}_2^+$  as the catalytic species suggests that other reactions catalyzed by In(III) species could also have cationic In(III) species as the real catalysts. DFT calculations revealed that the catalytic cycle of the cycloisomerization of 1,6-enynes catalyzed by  $\text{InCl}_3$  starts from  $\text{InCl}_2^+$  coordination to the alkyne of the substrate, generating a vinyl cation. Then nonclassical cyclopropanation of the vinyl cation to the alkene part of the substrate gives a homoallylic cation, which undergoes a novel homoallylic cation rearrangement involving a [1,3]-carbon shift to give the more stable homoallylic cation **15**. Finally  $\text{InCl}_2^+$  cation coordination assisted nonconjugated [1,2]-hydride shifts deliver the final nonconjugated diene products. The preference of generating nonconjugated dienes instead of conjugated dienes in the cycloisomerization reaction is mainly due to two reasons: coordination of the  $\text{InCl}_2^+$  to the alkene part in [1,2]-H shift transition states disfavors the conjugated [1,2]-H shifts that generate cations adjacent to the positively charged alkene, and coordination of  $\text{InCl}_2^+$  to the nonconjugated diene product is stronger than coordination to the conjugated diene, making nonconjugated [1,2]-H shift transition states lower in energy than conjugated [1,2]-H shift transition states, on the basis of the Hammond postulate. DFT calculations predicted that the conjugated [1,2]-H shifts could become favored if the electron-donating methyl substituent in the alkyne moiety of the 1,6-enyne is replaced by a H atom. This prediction of producing a conjugated diene has been verified experimentally. Rationalization about why type II rather than type I products were obtained using  $\text{InCl}_3$  as the catalyst in the cycloisomerization of 1,6-enynes has also been investigated computationally.



## INTRODUCTION

A great challenge facing today's studies of catalytic reactions is identifying the real catalytic species for the studied reactions. Recently Crabtree has summarized such challenges for many catalytic reactions in heterogeneous systems.<sup>1</sup> For many homogeneous catalytic reactions using either transition metals or main-group metals as catalysts, identifying the real catalytic species is also very challenging. One reason for this difficulty is the fact that impurities in the catalysts could be the real catalytic species.<sup>2</sup> One way to find the true catalytic metal of a homogeneous catalytic reaction is to do many carefully controlled experiments. If we are lucky, we could find the real catalytic metal(s) for the investigated reaction. Even though the real metal catalyst could be found by these control experiments, its real component and structure (for example, the oxidation state of the metal, the charge the real catalyst takes, the possible

ligands coordinated to the metal, the aggregation state of the catalytic species, etc.) could be still unknown. In this case, in principle, using state of the art ab initio calculations could help to find the exact structure of the real catalytic species, its charge, its ligands, and the oxidation state of the metal. Here calculations are used to compute all imaginable possibilities of the real catalytic species. Then we can rule out those possible catalytic species that give results contradictory to the experiments. If we are lucky again, we could find that only one proposed catalytic species satisfies almost all experimental results. In this case, a very possible catalytic species and its component and structure could be identified through the above computational and experimental investigations. To further confirm the real

Received: July 18, 2012

Published: August 29, 2012

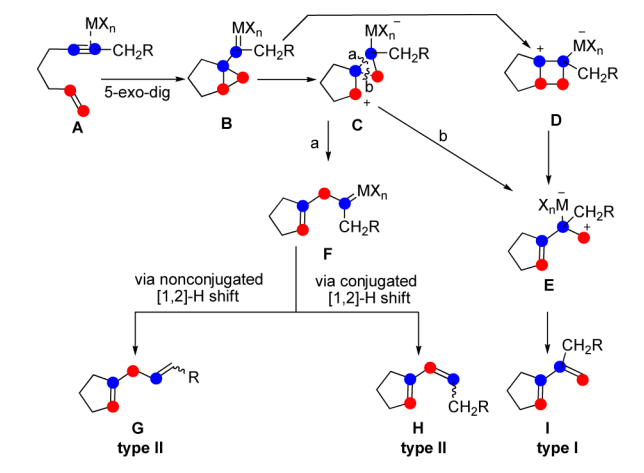
catalytic species, we can use calculations to predict new chemistry based on the identified catalytic species and use new experiments to test whether these predictions are correct or not. If the answer is yes again, we are further close to identifying the real catalytic species. Thanks to the tremendous advances in experimental techniques and computational chemistry, the chemistry community has been witnessing the fact that a combination of computational and experimental investigations of the reaction mechanisms has led to identifying many real catalytic species for many catalytic reactions.<sup>3</sup>

Even for a simple catalytic reaction using a single catalyst, identifying the real catalytic species and its exact form sometimes has also to rely on *ab initio* calculations to exclude some impossible candidates. For example,  $\text{InCl}_3$  or other  $\text{In(III)}$  species have been widely used as the catalyst for many reactions.<sup>4</sup> However, what are the real catalytic species for these catalytic transformations? Here we report our computational and experimental investigation of the mechanism and regiochemistry of the  $\text{InCl}_3$ -catalyzed cycloisomerization of 1,6-enynes. We show here that the real catalytic species of this reaction is  $\text{InCl}_2^+$  instead of the commonly regarded species  $\text{InCl}_3$  or its dimer. Such a discovery should prompt chemists to rethink other reactions catalyzed by either  $\text{In(III)}$  species or other Lewis acids such as  $\text{AlCl}_3$  and  $\text{GaCl}_3$ .<sup>5</sup>

## BACKGROUND

In recent decades, tremendous efforts have been devoted by chemists to the development of metal-catalyzed cycloisomerizations of enynes<sup>6</sup> because of the inherent atom economy, the easy preparation of the functionalized starting materials, and the facts that diverse products can be obtained selectively in these transformations by choosing appropriate catalysts. Among these transformations, skeletal reorganization of 1,6-enynes to provide diene products has drawn much attention from both synthetic and mechanistic points of view.<sup>7,8</sup> Depending on the nature of the catalysts and the substrates employed, the cycloisomerizations of 1,6-enynes can afford two kinds of diene products (Scheme 1). Consequently, the cycloisomerizations of

**Scheme 1. Proposed Mechanisms for Skeletal Reorganization of Enynes To Give Either Type I or Type II Diene Products**



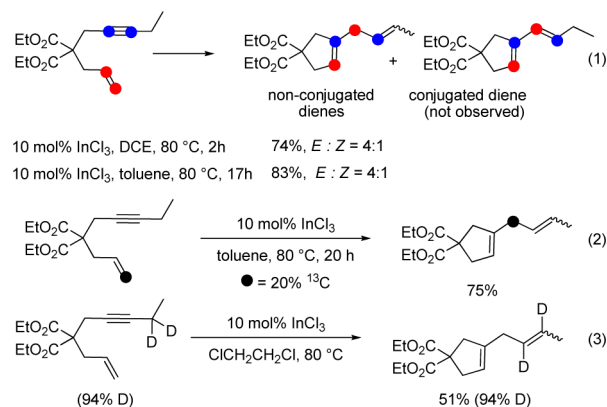
1,6-enynes are classified as either type I or type II cycloisomerization.<sup>9–17</sup> The type I cycloisomerization of 1,6-enynes gives conjugated dienes, which have the original two acetylenic

carbons connecting to each other in the internal positions of the diene moiety of the final products. The type II products from the 1,6-enyne cycloisomerization can be either conjugated or nonconjugated dienes, which have skeletal reorganized structures with the original connected acetylenic carbons inserted by the terminal ethylenic carbon.

It was proposed that both cycloisomerization pathways start with the activation of the alkyne of the 1,6-enyne, giving complex A. The activated alkyne in complex A resembles a vinyl cation, which is trapped by the nucleophilic alkene part of the enyne substrate, generating complex B in a [2 + 1] fashion. Complex B can be regarded as a zwitterionic or a metal carbenoid species. In type I cycloisomerization, intermediate B could be directly transformed to cyclobutane intermediate D, which undergoes ring opening and then dissociates the catalyst to afford the type I diene product I. In type II cycloisomerization, skeletal rearrangement of B, via double cleavage transformation, gives the spiro intermediate C, which then undergoes cleavage of the *a* bond (see Scheme 1 for bond labeling), to form intermediate F. A subsequent hydrogen shift and dissociation of the catalyst produce a skeletal reorganized type II diene, either G (via a nonconjugated [1,2]-H shift) or H (via a conjugated [1,2]-H shift), depending on the R group substituted in the yne part of the starting enyne substrate. It has also been proposed that cleavage of the *b* bond in the spiro intermediate C can give E, which then delivers the type I diene product I through liberation of the catalyst.

Today many catalysts have been used to catalyze the skeletal reorganization of enynes to give type II products since the first discovery of enyne cycloisomerization in 1987 by Trost.<sup>14</sup> Almost all catalysts give conjugated diene products, which are either type I or type II products. The only exception to this is the  $\text{InCl}_3$ -catalyzed cycloisomerization of 1,6-enynes,<sup>12a</sup> which gives nonconjugated type II dienes instead of conjugated dienes (Scheme 2). This type II enyne cycloisomerization was

**Scheme 2.  $\text{InCl}_3$ -Catalyzed Skeletal Reorganization of Enynes Reported by Chatani**



discovered by Chatani and co-workers.<sup>12</sup> Their experiments showed that nonconjugated dienes were generated when ene-internal-alkynes were used. (When an ene-terminal-alkyne was used, a type I diene product was found;<sup>12b</sup> in this study we only discuss cycloisomerizations of the ene-internal-alkynes. Therefore, unless specified directly, all discussed 1,6-enynes are referred to ene-internal-alkynes in the present paper.) The isotope labeling experiments also suggested that these reactions occur through the type II process (reaction 2 in Scheme 2), in

which a [1,2]-H shift occurs from the propargylic CH<sub>2</sub> moiety to the acetylenic carbon (reaction 3 in Scheme 2).

Given the prominent importance of enyne cycloisomerization in organic synthesis, computational studies on the reaction mechanisms are thus of fundamental interest for synthetic chemists who want to know how these reactions progress at the molecular level and understand the factors affecting these reactions' outcomes. To our knowledge, there have been only a few mechanistic studies reported so far for the enyne cycloisomerizations. Echavarren and co-workers explored the mechanism of Au-catalyzed skeletal reorganization processes that give types I and II and cyclohexene products using DFT calculations.<sup>7b,c</sup> The mechanisms of PtCl<sub>2</sub>- and GaCl<sub>3</sub>-mediated/catalyzed type I processes were also studied by Soriano<sup>7d,f</sup> and Yan, respectively.<sup>7i</sup> However, no mechanistic study of InCl<sub>3</sub>-catalyzed cycloisomerization has been explored to elucidate the reaction pathway, which is one of the main purposes of the present study. In addition to this, several key mechanistic issues listed below are worthy of further investigation.

The first and the most important question is as follows: which factors determine type II instead of type I regioselectivity of the InCl<sub>3</sub>-catalyzed cycloisomerization of 1,6-enynes?<sup>12</sup>

The second question, which puzzled us and was also the magnet greatly attracting our mechanistic curiosity, is about the generation of nonconjugated diene products when internal-alkyne-enes were used (Scheme 2). On the basis of the commonly accepted mechanisms shown in Scheme 1, we reasoned that the intermediate F in the type II reaction pathway can undergo two competitive [1,2]-H migration pathways. One is the migration of hydrogen from CH<sub>2</sub>R to give the experimentally observed nonconjugated diene G, and the other is the conjugated [1,2]-H migration pathway (F to H). Our chemical intuitions suggested that the conjugated [1,2]-H shifts should be easier both kinetically (due to the weaker allylic C–H bond) and thermodynamically (generation of conjugated diene should be much more stable), in comparison to nonconjugated [1,2]-H shifts, favoring generation of conjugated dienes.<sup>18</sup> Therefore, we were very curious to know why nonconjugated dienes rather than conjugated dienes were generated in the InCl<sub>3</sub>-catalyzed cycloisomerization.

The third question raised naturally after our understanding of the above issues is as follows: under what circumstances would the conjugated [1,2]-H shift process be favored with respect to the nonconjugated [1,2]-H shift? That is, can we reverse the H-shift selectivity through introducing some specific substitutes into the enyne substrates?

The fourth question is as follows: what is the real catalytic species of the InCl<sub>3</sub>-catalyzed reaction, InCl<sub>3</sub> or (InCl<sub>3</sub>)<sub>2</sub>? Answering this question is very important, not only for the present reaction but also for other InCl<sub>3</sub>-catalyzed reactions. In previous calculations on InCl<sub>3</sub>-catalyzed reactions, the investigators usually used InCl<sub>3</sub> as the catalytic species.<sup>19</sup> This could be wrong, and our study here could guide the future study of In chemistry.

Our DFT and experimental investigations on the above issues led us to propose that InCl<sub>2</sub><sup>+</sup> is the real catalytic species of the InCl<sub>3</sub>-catalyzed cycloisomerization. We have also used mass spectroscopy to confirm this. Of the same importance, rationalizations of this reaction's mechanism and selectivities (type I vs type II and conjugated [1,2]-H shifts vs nonconjugated [1,2]-H shifts) have been achieved through the present study. Further DFT prediction of the generation of conjugated type II diene product from InCl<sub>3</sub>-catalyzed

cycloisomerization of 1,6-enyne, which was based on the present mechanistic investigation, and experimental verification have also been carried out in this study.

## ■ COMPUTATIONAL METHODS

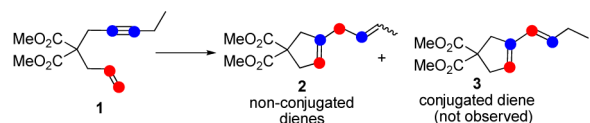
All calculations were performed with the Gaussian 03 program.<sup>20</sup> All gas-phase stationary points were optimized using the B3LYP<sup>21</sup> functional with the LANL2DZ<sup>22</sup> basis set and pseudopotential for the In atom and the 6-31G(d)<sup>23</sup> basis set for the other atoms (keyword SD was used in the calculations). Full Hessian matrixes in Gaussian 03 were calculated to verify the nature of all stationary points as either minima or first-order saddle points. The first-order saddle points were further characterized by intrinsic reaction coordinate (IRC)<sup>24</sup> calculations to confirm that the stationary points are correctly connected to the corresponding reactants and products. Solvation corrections to free energies were performed using UAHF radii and a CPCM<sup>25</sup> dielectric continuum solvent model in 1,2-dichloroethane (DCE). Solvation calculations were carried out on the gas-phase optimized structures. Bond order and atom charges were obtained by performing natural bond orbital (NBO)<sup>26</sup> calculations. All of the energies discussed in the paper and the Supporting Information are Gibbs free energies in the gas phase at 298 K ( $\Delta G_{\text{gas}}$ ).<sup>27</sup> Gibbs energies at 298 K in DCE solution ( $\Delta G_{\text{sol}}$ ) (here the entropies were approximated by using the gas-phase computed entropies) and the gas-phase enthalpies ( $\Delta H_{\text{gas}}$ ) are also provided for reference.

## ■ RESULTS AND DISCUSSION

**1. What Is the Real Catalytic Species of the InCl<sub>3</sub>-Catalyzed Cycloisomerization of 1,6-Enynes?** We computed the energy surface for 1,6-enyne cycloisomerization using both InCl<sub>3</sub> and (InCl<sub>3</sub>)<sub>2</sub> as the possible catalytic species. To our surprise, however, calculations by various methods such as using several different DFT functionals (B3LYP, M06, M06-2X, and MPW1K) and the MP2 method always favored generation of the conjugated dienes instead of nonconjugated dienes, in contrast to Chatani's experiments (see the Supporting Information). These contradicting calculation results suggest that neither InCl<sub>3</sub> nor (InCl<sub>3</sub>)<sub>2</sub> is the catalytic species for the InCl<sub>3</sub>-catalyzed cycloisomerization. In part 4 of this section, we will show that the preference for nonconjugated [1,2]-H shifts over conjugated [1,2]-H shifts is caused by the InCl<sub>2</sub><sup>+</sup> coordination to the alkene part of intermediate F (Scheme 1), which favors a cation coordination assisted nonconjugated [1,2]-H shift. The In–alkene coordination in intermediate F is absent when a neutral catalytic species, either InCl<sub>3</sub> or (InCl<sub>3</sub>)<sub>2</sub>, is proposed as the real catalyst, which prefers the conjugated [1,2]-H shifts.

It was found that InCl<sub>3</sub> crystallizes as a layered structure, consisting of a close-packed chloride arrangement with layers of In(III) centers, similar to the structure of AlCl<sub>3</sub>.<sup>28</sup> In solution, there were only reports of the structures of InCl<sub>3</sub> in CH<sub>3</sub>CN obtained by IR and Raman techniques from the Cho group.<sup>29a,b</sup> Cho found that InCl<sub>3</sub> in CH<sub>3</sub>CN is dissociated into a mixture of cations (CH<sub>3</sub>CN)<sub>x</sub>InCl<sub>2</sub><sup>+</sup> ( $x = 2-5$ ) and the anion InCl<sub>4</sub><sup>-</sup>. We speculated that, in both toluene and DCE solutions, the catalytic species could be InCl<sub>2</sub><sup>+</sup>, which is generated through the dissociation reaction  $2 \text{InCl}_3 = \text{InCl}_2^+ + \text{InCl}_4^-$  (certainly the generated InCl<sub>2</sub><sup>+</sup> could be further stabilized by coordinating to either the solvent or the substrate in the reaction system). To test this hypothesis, we carried out InCl<sub>3</sub>-catalyzed (20 mol %, entry b in Scheme 3) cycloisomerization of I in CH<sub>3</sub>CN, finding that the same products and the same ratio of products were obtained as those reactions in both toluene and DCE solvents, even though the conversion was low (10%). When the

### Scheme 3. Cycloisomerization of Enynes To Give Nonconjugated Type II Diene Products under Different Reaction Conditions



Entry	Reaction Conditions	Results
a.	10 mol% InCl <sub>3</sub> , DCE, 80 °C, 2h	74%, 2-E : 2-Z = 4:1 <sup>a</sup>
b.	20 mol% InCl <sub>3</sub> , CH <sub>3</sub> CN, 90 °C, 2h	conversion: 10% <sup>b</sup> , 2-E : 2-Z = 3:1 <sup>a</sup>
c.	150 mol% InCl <sub>3</sub> , CH <sub>3</sub> CN, 90 °C, 1h	conversion: 54% <sup>b</sup> , 2-E : 2-Z = 3:1 <sup>a</sup>
d.	400 mol% InCl <sub>3</sub> , CH <sub>3</sub> CN, 90 °C, 1h	conversion: 100% <sup>b</sup> , 2-E : 2-Z = 3:1 <sup>a</sup>
e.	10 mol% (AgX + InCl <sub>3</sub> ), DCE, 80 °C, 3h X = SbF <sub>6</sub> , BF <sub>4</sub> , OTf, OCOCF <sub>3</sub>	brsm <sup>c</sup> : 63% ~ 74%, 2-E : 2-Z = 3:1 <sup>a</sup> conversion: 55% ~ 83%
f.	10 mol% InI <sub>3</sub> , DCE, 80 °C, 2h	75%, 2-E:2-Z = 4:1 <sup>a</sup>

<sup>a</sup> the *E/Z* ratio was determined by GC.

<sup>b</sup> the products cannot be isolated on silica gel and conversion was determined by GC.

<sup>c</sup> brsm = based on the recovered starting material.

cycloisomerization reactions used the catalyst loadings of 150 mol % (entry c) and 400 mol % (entry d), the reaction conversions reached to 54% and 100% (determined by GC), respectively.

Electrospray ionization (ESI) mass spectrometry techniques have been widely used for the characterization of organometallic species. Koszinowski studied the heterolytic dissociation of allylindium(III) reagents, finding a series of species of  $\text{In}(\text{solvent})_m\text{X}_x\text{R}_{2-x}^+$  and  $\text{InX}_y\text{R}_{4-y}^-$  (solvent = DMF, THF, etc.; R = allyl; X = Cl, Br, I).<sup>30</sup> Electrospray ionization high-resolution mass spectroscopy (ESI-HRMS) of the insoluble precipitate from the resulting reaction mixture of 150 mol % InCl<sub>3</sub>-catalyzed cycloisomerization of **1** (Scheme 3 entry c) demonstrated the existence of the complexes  $(\text{InCl}_2+2)^+$  and  $(\text{InCl}_2+(2)_2)^+$  (Figure 1).<sup>31</sup> The counterion of the precipitate

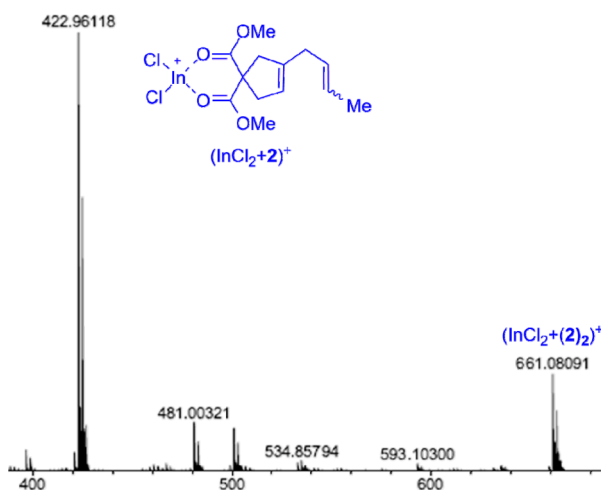


**Figure 1.** ESI-HRMS spectrum (positive mode) of the reaction mixture of 150 mol % InCl<sub>3</sub> mediated cycloisomerization of **1** in CH<sub>3</sub>CN (Scheme 3 in entry c) and the proposed structure.<sup>31</sup>

was found to be  $\text{InCl}_4^-$  (suggested by negative mode ESI-HRMS with  $m/z$  254.77980). We also found that, on increasing InCl<sub>3</sub> to 400 mol % in the cycloisomerization of **1** (entry d), only  $(\text{InCl}_2+2)^+$  can be detected by ESI-HRMS in the reaction mixture (without the signal of  $(\text{InCl}_2+(2)_2)^+$ ). These experiments gave more evidence to support the notion that  $\text{InCl}_2^+$  mediates the cycloisomerization when InCl<sub>3</sub> is used as the catalyst.

In acetonitrile solution, the cycloisomerization is not catalytic, in contrast to the InCl<sub>3</sub>-catalyzed cycloisomerizations in both DCE and toluene solvents. This is due to the low solubility of  $(\text{InCl}_2+2)^+$  in CH<sub>3</sub>CN. We found that the cycloisomerization reaction in DCE was homogeneous, while in CH<sub>3</sub>CN, the reaction system was heterogeneous with some insoluble species, which included  $(\text{InCl}_2+2)^+$ ,  $\text{InCl}_4^-$ , and other species, as demonstrated by ESI-HRMS spectroscopy (see the Supporting Information). In addition, we observed that the products **2** could not be isolated on silica gel through flash column chromatography, in contrast to the cases for the reactions in both DCE and toluene. Due to the insolubility of the product-catalyst complex  $(\text{InCl}_2+2)^+$  in CH<sub>3</sub>CN, the reaction can only occur stoichiometrically.<sup>32</sup>

DFT calculations indicated that InCl<sub>3</sub>-catalyzed cycloisomerization of 1,6-enynes in CH<sub>3</sub>CN is very possible, with reasonable activation barriers and thermodynamic data (see the Supporting Information). Interestingly, ESI-HRMS analysis of the reaction mixture of cycloisomerization of **1** by InCl<sub>3</sub> in DCE solution did not show the existence of the complex  $(\text{InCl}_2+2)^+$ . We hypothesized that, in DCE solution,  $\text{InCl}_2^+$  and  $\text{InCl}_4^-$  could recombine together to form InCl<sub>3</sub> again after the cycloisomerization reaction was finished.

In addition, we performed the same cycloisomerization using InCl<sub>3</sub> and AgX (X = SbF<sub>6</sub>, BF<sub>4</sub>, OTf, OCOCF<sub>3</sub>) together (Scheme 3, entry e), where cationic species were believed to be generated in situ.<sup>29c-e</sup> In these reactions, we observed the same *E/Z* ratios as those reported by Chatani and co-workers. This gives further support that cationic In species can catalyze the cycloisomerization. We observed here that counterions had effects on the reaction's conversions (the reasons for these observations are not known at this stage): when AgSbF<sub>6</sub>, AgOTf, AgBF<sub>4</sub>, and Ag(OCOCF<sub>3</sub>) were used in these reactions, the conversions (brsm) were 83% (63%), 73% (69%), 67% (73%), and 55% (74%), respectively.

In comparison to InCl<sub>3</sub>, InI<sub>3</sub> can dissociate more easily when a coordinating solvent (or a weak coordinating ligand) is present. For examples, X-ray analysis established that the compound  $\text{InI}_3(\text{Me}_2\text{SO})_2$  has the structure  $[\text{InI}_2(\text{Me}_2\text{SO})_4]\text{InI}_4^-$ ,<sup>33a</sup> vibrational spectroscopy indicated that  $[\text{InI}_2(\text{CH}_3\text{CN})_4]\text{InI}_4^-$ <sup>33b</sup> exists in the solid state. In both cases, the NMR results supported the presence of the  $\text{InI}_4^-$  anion in solution.<sup>33c</sup> It was also reported that, in the presence of rigid chelate ligands (L-L), indium(III) halides (InCl<sub>3</sub>, InBr<sub>3</sub>, and InI<sub>3</sub>) easily produce distorted-tetrahedral cations of  $[\text{InX}_2(\text{L-L})][\text{InX}_4^-]$  (X = Cl, Br, I).<sup>34</sup> These ionic species were determined by X-ray analysis and are stable in noncoordinating solvents.<sup>34</sup> All these reports suggested that InI<sub>3</sub> (and InCl<sub>3</sub>) disassociates very easily in solution, especially when some ligands are present. Herein, we propose that the 1,6-enyne can be regarded as an alkene/alkyne bidentate ligand that helps the dissociation of InI<sub>3</sub>. This complexation leads to the generation of  $[\text{InX}_2(\text{ene-yne})]^+$  in the reaction. To further support our hypothesis, we used InI<sub>3</sub> (10 mol %) as a catalyst for the cycloisomerization of **1** in DCE solution at 80 °C and found that 75% of **2** (2-E:2-Z = 4:1) was obtained within 2 h (Scheme 3, entry f). This result is very close to the result from the reaction catalyzed by InCl<sub>3</sub>, giving further evidence that the real catalytic species is  $\text{InCl}_2^+$  in the InCl<sub>3</sub>-catalyzed cycloisomerization.

In summary, our experimental results revealed that the catalytic species in the InCl<sub>3</sub>-catalyzed cycloisomerization of 1,6-enynes is  $\text{InCl}_2^+$ . This is also supported by the DFT calculations, which are given below (for additional discussion of the

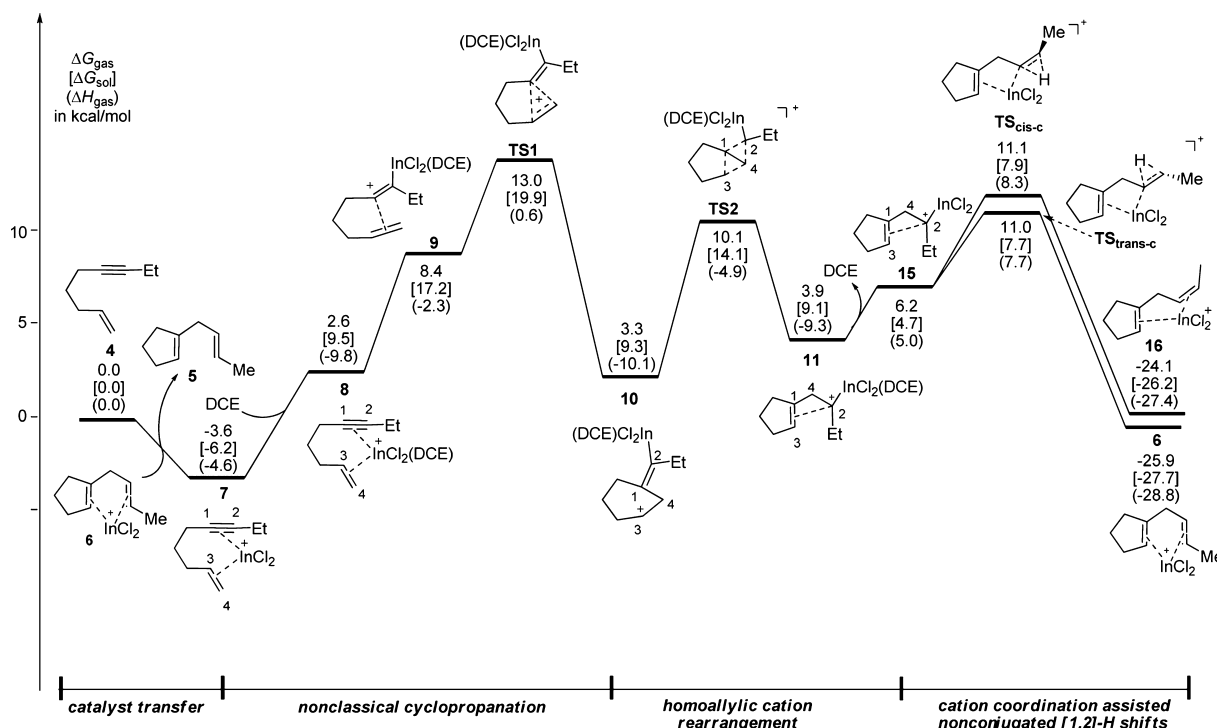
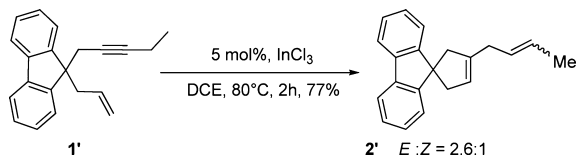


Figure 2. Energy surface of the cycloisomerization reaction of enyne with  $\text{InCl}_2^+$  as the catalytic species in DCE solution.

dissociation processes using DFT calculation results, see the Supporting Information).<sup>35</sup>

**2. Energy Surface of the Catalytic Cycle of Cycloisomerization using  $\text{InCl}_2^+$  as the Catalytic Species.** To reduce the cost of calculations without sacrificing the reliability of the mechanistic study, we computed the catalytic cycle of the type II cycloisomerization of model substrate **4** using  $\text{InCl}_2^+$  as the real catalytic species (Figure 2). We must emphasize here that the model reaction of **4** can mimic the real substrates in Chatani's experiments, which have either diester or disulfonate as their tethers.<sup>12</sup> In Chatani's cycloisomerization reaction, we found computationally that not only the ene and yne parts but also the tethers can coordinate to the catalytic species,  $\text{InCl}_2^+$ . Despite this, we believe that coordination of the tether to some catalyst species could affect the reaction rate but not the mechanism of the cycloisomerization reaction. To test this speculation, we synthesized substrate **1'** (Scheme 4), which does not

**Scheme 4.  $\text{InCl}_3$ -Catalyzed Cycloisomerization of **1'** Using the Reaction Conditions Reported by Chatani**



have the tether coordination to the catalyst (in this case, there is also a possibility that some  $\text{InCl}_2^+$  coordinates to the benzene ring through the cation- $\pi$  interaction). Our experiment found that the type II nonconjugated product **2'** ( $E:Z = 2.6:1$ ) was obtained when the same reaction conditions used by Chatani were applied.<sup>36</sup> Therefore, the DFT study of the model reaction of **4** can be used to explain the general mechanism of the 1,6-enyne isomerizations catalyzed by  $\text{InCl}_3$ .

Figure 2 gives the DFT computed energy surface of the catalytic cycle, which starts with the formation of  $\text{InCl}_2^+$ -substrate complex **7**, followed by a nonclassical cyclopropanation, homoallylic cation rearrangement, and the cation coordination assisted nonconjugated [1,2]-H shift processes. In what follows, we will depict each step in more detail. Then in parts 3 and 4 of this section, we will analyze respectively why type II instead of type I cycloisomerization takes place and why nonconjugated type II diene products are formed.

**Nonclassical Cyclopropanation Step.** The  $\text{InCl}_2^+$ -catalyzed cycloisomerization cycle starts with the catalyst transfer between catalyst-product complex **6** (here we only use **6** to elucidate this process; similarly, **16** undergoes the same process to give rise to **7**), generated from the previous catalytic cycle, and the enyne substrate **4** (Figures 2 and 3). The catalyst transfer step is exergonic by 3.6 kcal/mol, giving intermediate **7**, in which the catalyst coordinates to both the triple and double bonds of the enyne. Complex **7** is  $\eta^4$  coordinated, with the distances of In to C1, C2, C3, and C4 of 2.47, 2.63, 2.77, and 2.50 Å, respectively.

Coordination of the In atom in complex **7** by a solvent molecule,<sup>37</sup> dichloroethane (DCE), leads to the formation of the  $\eta^5$  complex **8**. Complex **8** is more stable than **7** by 5.2 kcal/mol in terms of enthalpy in the gas phase, but in terms of Gibbs free energy, the former is less stable than the latter by 6.2 kcal/mol, due to the entropy penalty of this coordination process. To continue the cycloisomerization process, complex **8** liberates the coordinated alkene part, generating the less stable complex **9**. In **9**, the coordinated alkyne part can be regarded as a vinyl cation, which is stabilized through the weak coordination of the liberated alkene moiety of the substrate, as demonstrated by the bond distances of C1-C3 (3.00 Å) and C1-C4 (3.37 Å). Intermediate **9** then undergoes an intramolecular nucleophilic attack (nonclassical cyclopropanation) of the alkene toward the vinyl cation via **TS1** to give the more stable intermediate **10**,

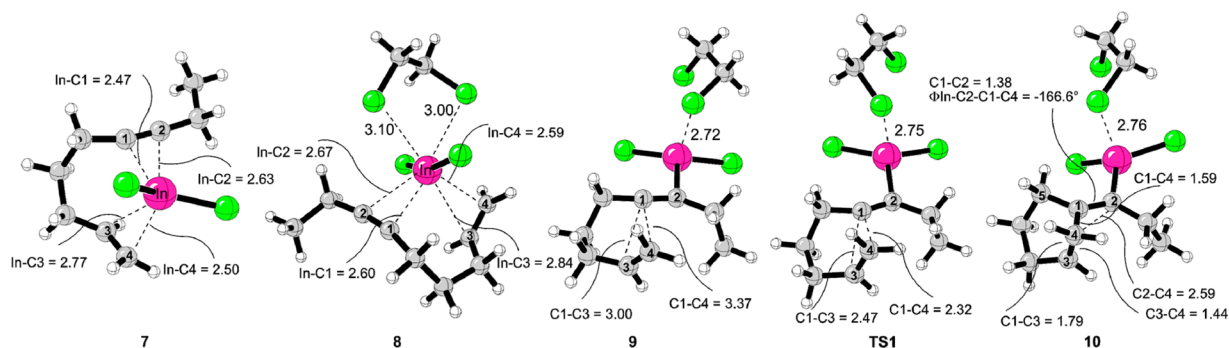


Figure 3. Selected DFT computed structures involved in the nonclassical cyclopropanation step (distances in Å).

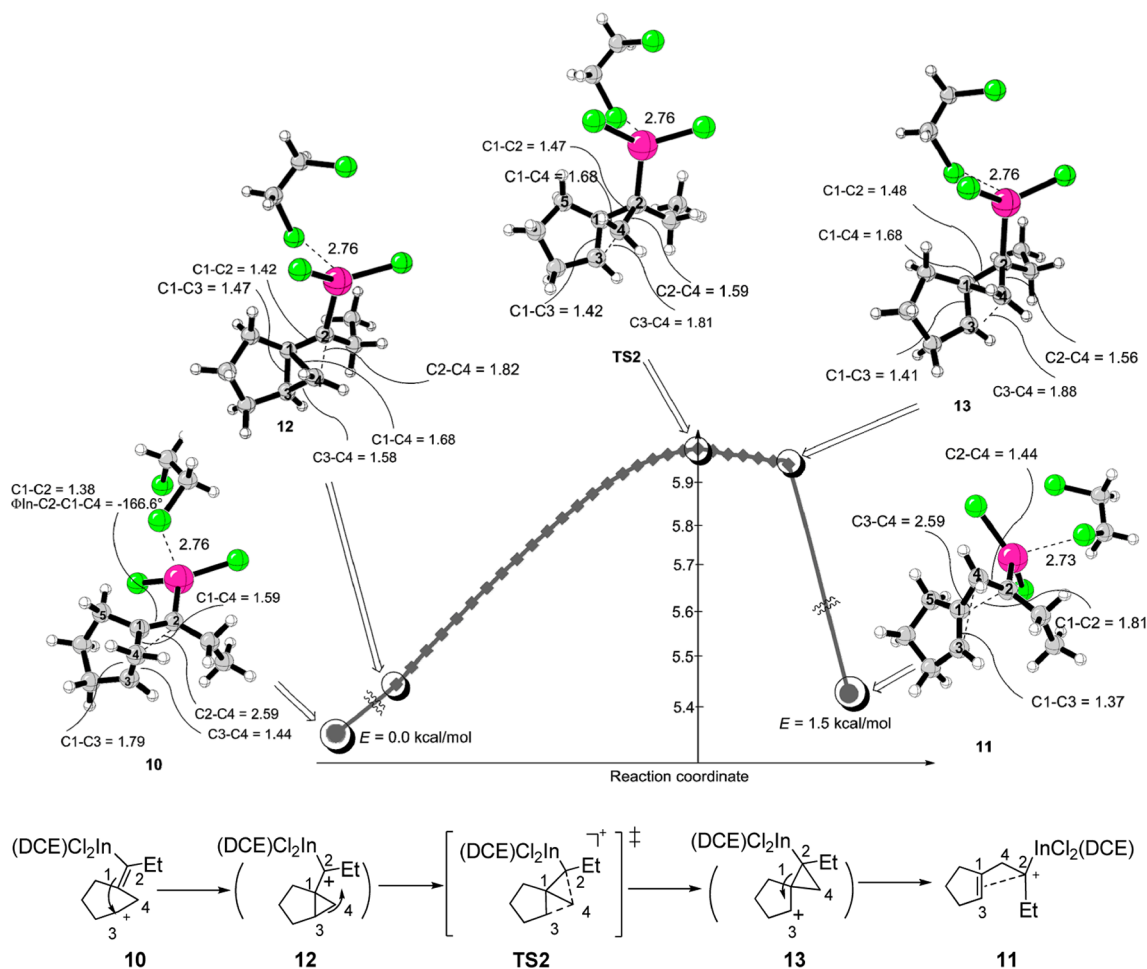
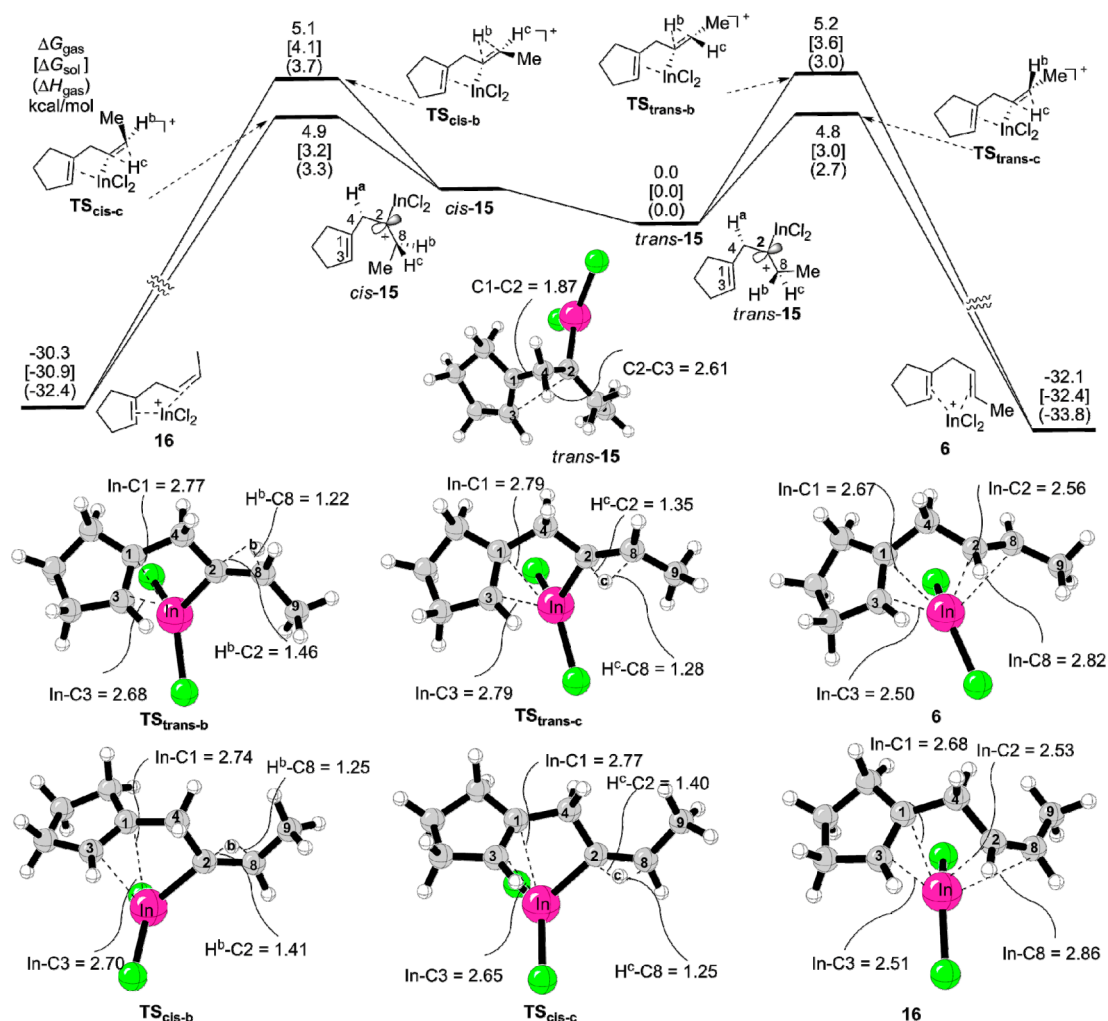


Figure 4. IRC path from TS2 of the homoallylic cation rearrangement process (distances in Å). Energies given here are electronic energies without ZPE corrections.

which can be regarded as a homoallylic cation, or a nonclassical cyclopropane (therefore, we call this process as a nonclassical cyclopropanation process) (Figure 3). The overall activation free energy of the generation of the homoallylic cation is 16.6 kcal/mol in the gas phase (from 7 to TS1), and the rate-determining transition state is the nonclassical cyclopropanation transition state TS1.

**Homoallylic Cation Rearrangement.** The following step is the rarely encountered homoallylic cation rearrangement, converting homoallylic cation 10 to another homoallylic cation 11 via transition state TS2.<sup>38</sup> A similar process has been studied by Echavarren and co-workers, and this was called a double-cleavage

mechanism due to the simultaneous cleavages of the C1–C2 and C3–C4 bonds in this process.<sup>7c</sup> After analyzing the structures involved in this process, we thought that it is best to describe the present process as a homoallylic cation rearrangement process (Figure 4). In 10, the C1–C2 (1.38 Å) and C1–C4 (1.59 Å) bonds can be characterized as a double bond and a single bond, respectively, while the C1–C3 bond is not well formed (1.79 Å). Therefore, 10 can be regarded as a homoallylic cation (or a nonclassical cyclopropylcarbanyl cation). The homoallylic cation rearrangement starts from formation of the C1–C3 bond to give the cyclopropylcarbanyl cation 12, which then undergoes a [1,3]-carbon sigmatropic shift via TS2



**Figure 5.** Relative energies of the nonconjugated [1,2]-H shifts together with the DFT computed structures of the key stationary points involved in these processes (distances in Å).

to give another cyclopropylcarbanyl cation 13. During the [1,3]-carbon shift, it is the distal C3–C4 bond that breaks and the C2–C4 bond that forms. Intermediate 13 then breaks its C1–C2 bond to give the homoallylic carbocation 11.

Support of our description of the homoallylic rearrangement from 10 to 11 can be appreciated from IRC<sup>24</sup> calculations (Figure 4), which showed that TS2 is connected to “intermediates” 12 and 13. Here, 12 and 13 are not the stationary points in the energy surface, because geometry optimizations of 12 and 13 directly gave intermediates 10 and 11, respectively.

**Cation Coordination Assisted Nonconjugated [1,2]-H Shift Processes.** The next step in the catalytic cycle is the [1,2]-H shift step. This could start from 11 directly or commence from desolvation of the solvent to give 15, which then undergoes [1,2]-H shift processes. Our calculations found that the latter is more favored, giving the experimentally observed nonconjugated dienes. Therefore, we here mainly discuss how these favored hydrogen shifts occur.

Intermediate 15, like intermediate 11, has a weak interaction between C2 and the C1=C3 bond (Figure 5). 15 has the methyl group and the cyclopentenyl ring in the trans configuration to minimize the steric repulsion (here we label this conformer as *trans*-15). Another conformer, *cis*-15, with the methyl group and the cyclopentenyl ring in proximity, is not an energy minimum. In *trans*-15, both H<sup>b</sup> and H<sup>c</sup> atoms can

undergo [1,2]-H shift processes to give the trans nonconjugated dienes. H<sup>b</sup> and H<sup>c</sup> in *cis*-15 can also take part in the [1,2]-H shifts, but in this case, they will give cis nonconjugated dienes. All four nonconjugated [1,2]-H shift transition states from *cis*- and *trans*-15 were located, showing that they are very close in energy and suggesting that both cis and trans nonconjugated dienes will be generated. This is consistent with experimental observations (*E*:*Z* = 4:1 in Scheme 2 and *E*:*Z* = 2.6:1 in Scheme 4). All of these nonconjugated [1,2]-H shifts occur easily, with activation free energies of around 5 kcal/mol, and are more favored than the conjugated [1,2]-H shift processes (see below).<sup>39,40</sup> In the [1,2]-H shift transition states, the C1=C3 bonds are coordinated by the cationic InCl<sub>2</sub><sup>+</sup> species, and we call these reactions cation coordination assisted nonconjugated [1,2]-H shifts (a detailed discussion is given in part 4 of this section).

From the above discussion of the mechanism, it is concluded that the InCl<sub>3</sub>-catalyzed cycloisomerization reaction of enynes starts with formation of the InCl<sub>2</sub><sup>+</sup>-substrate complex 7, followed by nonclassical cyclopropanation, which is the rate-determining step of the reaction with an activation free energy of 16.6 kcal/mol in the gas phase. Via a novel homoallylic cation rearrangement involving a [1,3]-carbon shift, another homoallylic cation 15, the precursor of the following [1,2]-H shifts, is obtained. Finally, easy cation coordination assisted

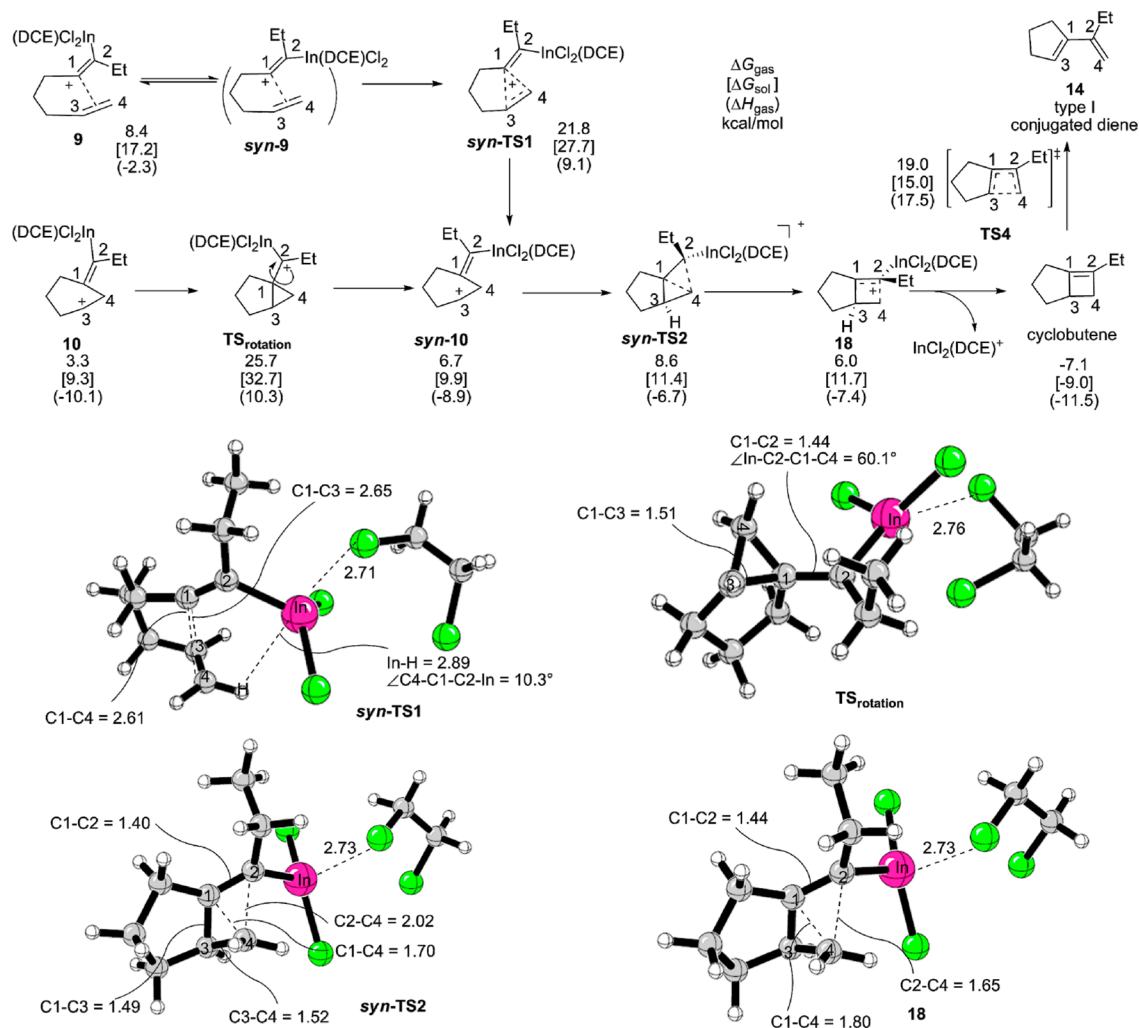


**Figure 6.** Relative energies of the disavored pathways leading to the type II diene product together with several key structures involved in these processes (distances in Å).

nonconjugated [1,2]-H shifts give a mixture of cis and trans nonconjugated dienes. In DCE solution, calculations found that the overall activation free energy of the cycloisomerization is 26.1 kcal/mol (from 7 to TS1), consistent with the experimental observation that heating the InCl<sub>3</sub>-catalyzed cycloisomerization reaction mixture at 80 °C is required.

**3. Why Are Type II but not Type I Products Generated?** Figure 2 gives the energy surface of the experimentally observed pathway leading to the type II cycloisomerization. Here we present other two possible competitive pathways leading to the type I cycloisomerization of 1,6-enynes using InCl<sub>2</sub><sup>+</sup> as the catalyst (Figure 6).

One possible pathway for the generation of the type I products starts from an alternative complexation process between InCl<sub>2</sub><sup>+</sup> and the substrate, giving *syn-9* instead of 9 (Figure 6). The hypothetical *syn-9*, which is not a minimum, has the ethyl and the tether group in a cis configuration, while 9 has these two groups in a trans configuration. *syn-9* can also undergo cyclopropanation (*syn-TS1*), giving the homoallylic cation *syn-10*. *syn-10* differs from 10 (Figure 2) in the relative conformation of the C1=C2 bond. Then C1-C3 bond formation and a [1,2]-carbon sigmatropic shift converts *syn-10* to intermediate 18, which can then give the type I product 14 through further steps.<sup>7d,e</sup> Unfortunately, this pathway from 9 to 14 is

disavored by 8.8 kcal/mol in comparison with the pathway leading to a type II diene product (*syn-TS1* vs TS1; see Figures 2 and 6). The inferior *syn* cyclopropanation step is attributed to the steric repulsion encountered between the double bond and inner catalyst, which hinders C1-C3 and C1-C4 bond formations. For example, in *syn-TS1*, the distance from the In atom to the inner H atom at C4 is 2.89 Å and the C4-C1-C2-In dihedral angle is 10.3°, indicating a repulsion between In and the cyclopropane moiety. The structures of *syn-TS1* and TS1 also reflect this repulsion in that the former is an early transition state in comparison to the latter: the forming C1-C3 and C1-C4 bonds are 2.65 and 2.61 Å in *syn-TS1*, while they are 2.47 and 2.32 Å in TS1.

Another possible pathway to the type I product begins with the rotation of the C1=C2 double bond in intermediate 10 to give *syn-10*, which can then give type I product as well (Figure 6). A similar rotation process was computed by Echavarren in Au-catalyzed cycloisomerization. However, this bond rotation (via TS<sub>rotation</sub>), requiring an activation energy of 29.3 kcal/mol, is not favored in comparison to the homoallylic rearrangement and [1,2]-H shift processes in the pathway of generating type II nonconjugated dienes, which occur easily with activation free energies of less than 14.6 kcal/mol. The difficulty associated

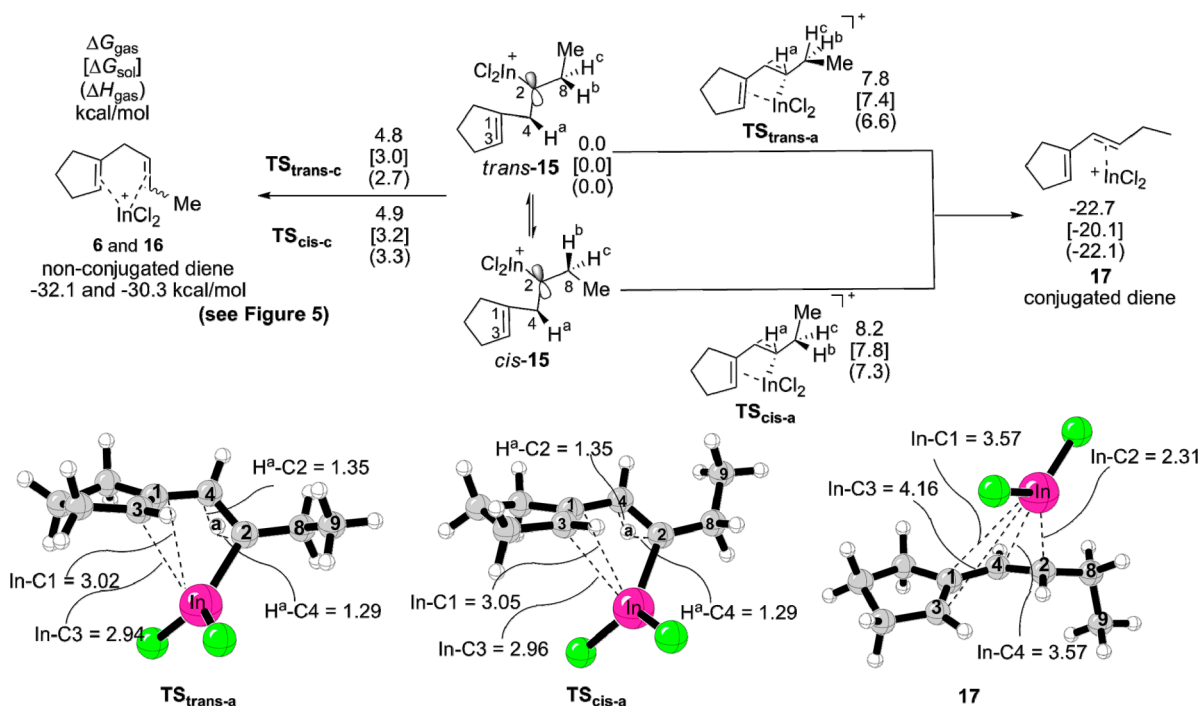
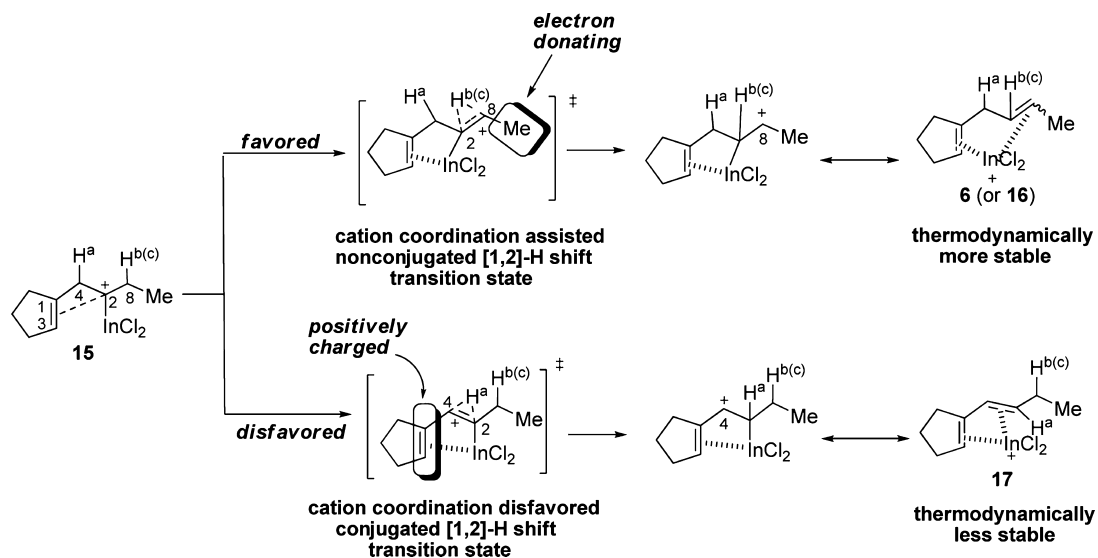


Figure 7. Relative energies of the nonconjugated [1,2]-H shift pathways and the corresponding transition states and products (distances in Å).

#### Scheme 5. Rationalization of Regioselectivity of the [1,2]-H Shifts from 15



with this rotation can be attributed to the double-bond character of  $\text{C}1=\text{C}2$  in **10** (1.38 Å; see Figure 4).

**4. Why Are Nonconjugated instead of Conjugated Dienes Generated? Rationalization, Prediction, and Experimental Verification.** *Rationalization.* In the type II pathway, we only discussed nonconjugated [1,2]-H shift processes that generate the experimentally observed nonconjugated diene products. In addition to these, there should be other two competitive conjugated [1,2]-H shift processes involving the migration of the allylic hydrogen atoms ( $\text{H}^{\text{a}}$  atoms) in **15** (Figure 7). Two transition states,  $\text{TS}_{\text{trans-a}}$  and  $\text{TS}_{\text{cis-a}}$  for these two competitive [1,2]-H shifts were located, showing that they are about 3 kcal/mol higher in terms of Gibbs free energy than the nonconjugated [1,2]-H shift transition states with  $\text{H}^{\text{b}}$  and  $\text{H}^{\text{c}}$  as the migrating atoms. This indicates that only

nonconjugated dienes are generated exclusively, consistent with Chatani's experiments. However, chemical intuition suggested that the conjugated [1,2]-H shifts should be favored both kinetically (allylic C–H bond is weaker)<sup>18</sup> and thermodynamically (conjugated diene should be much more stable), in comparison to nonconjugated [1,2]-H shifts, making generation of conjugated dienes favored. Therefore, what are the reasons for this selectivity?

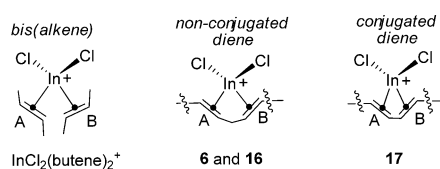
Two reasons can explain why conjugated [1,2]-H shifts are disfavored compared with the nonconjugated [1,2]-H shifts. In Scheme 5, intermediate **15** can be regarded as a C2 carbocation, where a positive charge resides in the C2 atom and the In center. In both conjugated and nonconjugated [1,2]-H shift transition states, the  $\text{C}1=\text{C}3$  bonds coordinate to the positively charged cationic  $\text{InCl}_2^+$ , suggesting that the C1 and C3

atoms of the alkene parts in the five-membered rings of these transition states have some positive charges. Conjugated [1,2]-H shifts will generate positive charges at the C4 atoms in the corresponding transition states and the final products. The cationic C4 atoms in these structures are adjacent to the positively charged C1 and C3 atoms coordinated to  $\text{InCl}_2^+$ , disfavoring the conjugated [1,2]-H shifts. In contrast, the positive charge generated at the C8 atom in the transition states of nonconjugated [1,2]-H shifts can be stabilized by the electron-donating methyl group attached at the C8 atom, favoring the corresponding [1,2]-H shifts kinetically. The nonconjugated [1,2]-H shifts are favored due to  $\text{InCl}_2^+$  cation coordination. Therefore, we call these processes cation coordination assisted nonconjugated [1,2]-H shifts.

Another reason for the above preference can be explained by the Hammond postulate.<sup>42</sup> It is generally believed that a more exothermic reaction has an earlier transition state and lower activation energy in comparison to a less exothermic reaction. Our calculations found that  $\text{InCl}_2^+$  coordinates to nonconjugated dienes much more strongly than conjugated diene products by ca. 10 kcal/mol. This suggests that nonconjugated [1,2]-H shift transition states are more stabilized with respect to its counterparts, according to the Hammond postulate. We point out here that, without coordination of  $\text{InCl}_2^+$ , the final conjugated diene product is more stable than the nonconjugated diene by 14.5 kcal/mol. However, this thermodynamic nature does not reflect the [1,2]-H shift processes with  $\text{InCl}_2^+$  catalyst present, which prefer to generate the thermodynamically more stable nonconjugated diene catalyst complexes. This reflects the effect of cation coordination to the final dienes, affecting the reaction's thermodynamics (and also kinetics, on the basis of the Hammond postulate).

The relative stability of  $\text{InCl}_2^+$  complexes with nonconjugated and conjugated dienes is due to the geometry. The cationic In(III) metal in  $\text{InCl}_2(\text{butene})_2^+$  adopts a tetrahedral configuration (Scheme 6). Calculations found that the alkene–

### Scheme 6. Rationalization of Relative Complexations of $\text{InCl}_2^+$ with Various Diene Ligands by Considering Relative Binding Angles and Energies



	$\text{InCl}_2(\text{butene})_2^+$	6	16	17
$\angle \text{A-In-B}$	114.6°	81.2°	78.1°	35.0°
binding energy <sup>a</sup> (kcal/mol)	-75.2	-73.6	-73.6	-58.4

<sup>a</sup> binding energy = enthalpy( $\text{InCl}_2^+$ -diene) - enthalpy(diene) - enthalpy( $\text{InCl}_2^+$ )

In–alkene angle in  $\text{InCl}_2(\text{butene})_2^+$  is 114.6°. However, complex 6, which has the two coordinated alkenes connected to each other, is greatly distorted with an alkene–In–alkene angle of 81.2°, dramatically less than the optimal angle in  $\text{InCl}_2(\text{butene})_2^+$ . This distortion is further increased in complex 17 with conjugated diene as the coordination ligand, as demonstrated by the alkene–In–alkene angle of 35.0° in 17. Cation In(III) binds much more strongly to nonconjugated diene than to conjugated diene, reflecting this thermodynamic preference (73.6 vs 58.4 kcal/mol). Consequently,  $\text{InCl}_2^+$  prefers to coordinate to the nonconjugated diene over the conjugated diene.

The above calculation results showed that cationic  $\text{InCl}_2$  coordination to the C1=C3 bond in the [1,2]-H shift transition

states is very critical to favor the nonconjugated [1,2]-H shift. However, if  $\text{InCl}_3$  or  $(\text{InCl}_3)_2$  is proposed as the real catalyst, conjugated diene will be generated, in contrast to Chatani's experiments. This is because  $\text{InCl}_3$  or  $(\text{InCl}_3)_2$  is neutral and the C=C bond in the five-membered ring of intermediate F (Scheme 1) is not coordinated to the In metal. Consequently, the above effects introduced by the cationic In species coordination are absent in the [1,2]-H shift transition states when the competing nonconjugated and conjugated [1,2]-H shifts are compared. In these cases using neutral catalytic species, conjugated [1,2]-H shifts are favored both kinetically and thermodynamically (the results are summarized in the Supporting Information).

**DFT Prediction and Experimental Verification of the Generation of Conjugated Type II Diene.** On the basis of the mechanistic insights shown in Scheme 5, we then predicted that, through introducing a different R group, we could tune the conjugated [1,2]-H shifts into favored ones with respect to the nonconjugated [1,2]-H shifts in terms of activation energy (Scheme 7a). Our transition state models suggest that an electron-donating group (methyl) connecting to C8 is crucial in stabilizing the hydride shift transition states (Scheme 5). We reasoned that changing the methyl group (in C8) to a hydrogen atom (a much weaker electron-donating group) could switch the previous selectivity.

To our delight, DFT calculations supported our hypothesis, showing that generation of conjugated diene is favored in comparison to the nonconjugated [1,2]-H shifts (Scheme 7a). To prove this prediction, we synthesized the methyl-substituted enyne 19 and treated it with  $\text{InCl}_3$  in DCE. To our excitement, we isolated the computationally predicted conjugated type II diene product 21<sup>43</sup> (only the trans isomer<sup>41</sup> was obtained). In addition, type I diene 20 was also obtained (the ratio of the two products 20 and 21 is 1:1.1, as determined by <sup>1</sup>H NMR spectroscopy and GC of the reaction mixture). Further DFT calculations after the experimental test found that generation of the type I conjugated diene 20 from 22 is due to the competitive C1–C4 cleavage pathway from intermediate 22 (details of the calculated energy surface and structures are summarized in the Supporting Information).<sup>44</sup> The success in obtaining conjugated diene 21 provides further support of the reaction mechanism shown in Figure 2.

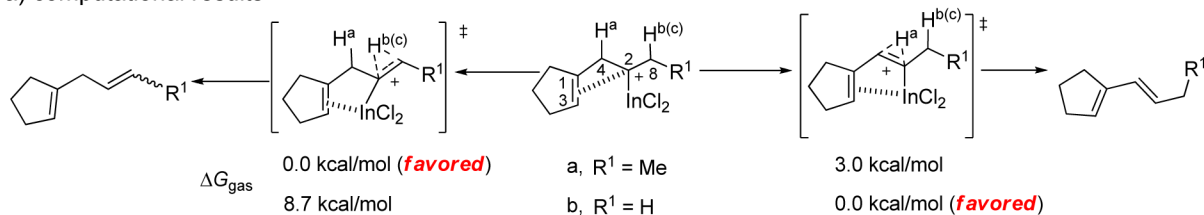
## CONCLUSIONS

In conclusion, through DFT calculations and a new experimental investigation of the mechanism and regioselectivity of  $\text{InCl}_3$ -catalyzed cycloisomerization reactions of 1,6-enynes, we propose that the catalytic species of this reaction is the in situ generated  $\text{InCl}_2^+$ . Further ESI-HRMS identified the existence of  $\text{InCl}_2^+$  in acetonitrile solution. This finding of  $\text{InCl}_2^+$  as the catalytic species suggests that other reactions catalyzed by In(III) species could also have cationic In(III) species as the real catalysts.

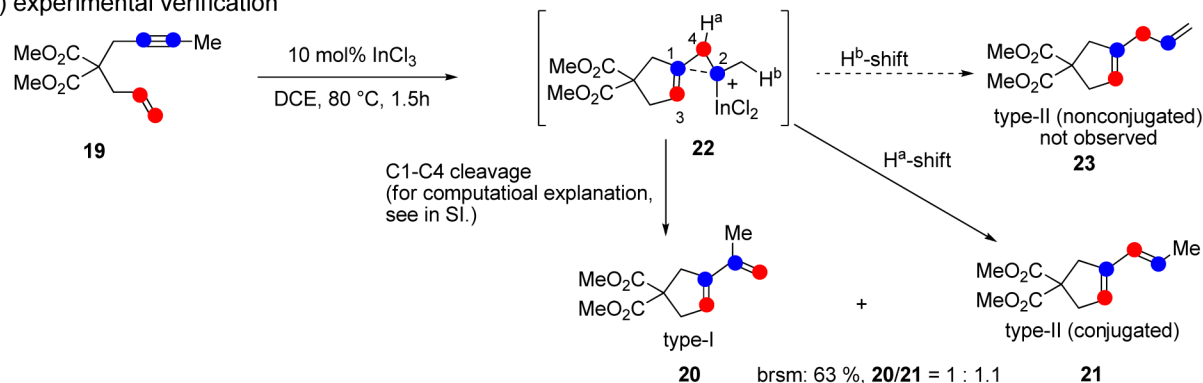
In addition, detailed information on the energies and structures of the stationary points involved in the catalytic cycle of the 1,6-enyne cycloisomerization catalyzed by  $\text{InCl}_3$  has been obtained (Figure 2). DFT calculations found that the catalytic cycle of the cycloisomerization starts from  $\text{InCl}_2^+$  coordination to the alkyne of the substrate, generating a vinyl cation. Then nonclassical cyclopropanation of the vinyl cation to the alkene part of the substrate gives a homoallylic cation (a nonclassical cyclopropane), which undergoes a novel homoallylic cation rearrangement involving a [1,3]-carbon shift to give another homoallylic cation 15. Finally,  $\text{InCl}_2^+$  cation

Scheme 7. (a) Calculation Predicted Selectivities of the [1,2]-H Shifts with Different Substituents at C8 and (b) InCl<sub>3</sub>-Catalyzed Cycloisomerization of 19, Giving Conjugated Diene Products

## a) computational results



## b) experimental verification



coordination assisted nonconjugated [1,2]-H shifts deliver the nonconjugated diene products. The preference for generating nonconjugated dienes over conjugated dienes is mainly due to two reasons: coordination of the InCl<sub>2</sub><sup>+</sup> to the alkene part in [1,2]-H shift transition states disfavors the conjugated [1,2]-H shifts that generate cations adjacent to the positively charged alkene, and coordination of InCl<sub>2</sub><sup>+</sup> to the nonconjugated diene product is stronger than coordination to the conjugated diene, making nonconjugated [1,2]-H shift transition states lower in energy than conjugated [1,2]-H shift transition states on the basis of the Hammond postulate. In addition to the mechanistic insights, DFT calculations predicted that the conjugated [1,2]-H shift selectivity could be switched when replacing the electron-donating methyl group (which helps the nonconjugated [1,2]-H shifts) to a hydrogen atom. This prediction of producing conjugated diene has been verified experimentally. Type II rather than type I product formation can be understood by the preference of trans-cyclopropanation of the vinyl cation to the alkene part of the enyne substrate, which leads to type II products (Figure 6).<sup>46</sup>

## EXPERIMENTAL SECTION

Anhydrous solvents (THF, CH<sub>3</sub>CN, DCE, and CH<sub>2</sub>Cl<sub>2</sub>) were obtained by distillation after treating them with appropriate dehydration reagents. The reaction course was followed by TLC (petroleum ether–ethyl acetate) and GC analyses. Purification of the resulting mixture involved concentration under vacuum and chromatographic separation by using silica gel. All NMR spectra were recorded on a 400 MHz spectrometer. <sup>1</sup>H and <sup>13</sup>C NMR spectra were recorded using the deuterated solvent as the lock and the residual solvent as the internal reference. High-resolution mass spectra (HRMS) were performed by the ESI ionization technique (using a quadrupole analyzer).

**Synthesis of Dimethyl 2-Allyl-2-(pent-2-ynyl) malonate (1).** To a suspension of NaH (0.16 g, 6.6 mmol, washed with hexane) in 10 mL of THF was added dropwise dimethyl 2-allylmalonate<sup>7b</sup> (1.23 g, 5.5 mmol) at 0 °C over a period of 15 min. Then the mixture was stirred at room temperature until the evolution of hydrogen gas subsided. The mixture was cooled to 0 °C, and a solution of 1-bromopent-2-yne (0.88 g, 6.0 mmol) was added dropwise over a period of 15 min.

After the mixture was stirred for an additional 12 h at room temperature, water was added slowly at 0 °C, and the organic layer was separated. The aqueous layer was extracted with Et<sub>2</sub>O, and the combined organic layers were washed with brine, dried over Na<sub>2</sub>SO<sub>4</sub>, and concentrated under vacuum. The residue was purified by column chromatography on silica gel (eluted with PE/EA 30/1) to give **1** as a colorless oil (2.27 g) in 72% yield. **1**: colorless oil; <sup>1</sup>H NMR (400 MHz, CDCl<sub>3</sub>)  $\delta$  5.64 (m, 1H), 5.16 (d, *J* = 17.0 Hz, 1H), 5.12 (d, *J* = 10.2 Hz, 1H), 3.73 (s, 6H), 2.79 (d, *J* = 7.5 Hz, 2H), 2.75 (s, 2H), 2.13 (q, *J* = 7.4 Hz, 2H), 1.09 (t, *J* = 7.5 Hz, 3H); <sup>13</sup>C NMR (101 MHz, CDCl<sub>3</sub>)  $\delta$  170.5, 132.0, 119.5, 85.1, 73.5, 57.3, 52.6, 36.6, 23.0, 14.2, 12.3; FT-IR (neat):  $\nu$  1739, 1441, 1296, 1241 cm<sup>-1</sup>; HRMS (ESI) calcd for C<sub>13</sub>H<sub>18</sub>NaO<sub>4</sub> [*M* + Na<sup>+</sup>] 261.1101, found 261.1097.

**Synthesis of 9-Allyl-9-(pent-2-ynyl)-9H-fluorene (1').** A hexane solution of <sup>n</sup>BuLi (3.0 mL, 1.6 M, 4.8 mmol) was added to a solution of 9-allyl-9H-fluorene<sup>45</sup> (500 mg, 2.42 mmol) in THF (20 mL) at 0 °C. The resulting slurry was warmed to 25 °C and stirred for 2 h. The solution was cooled to -78 °C, and 1-bromopent-2-yne (462 mg, 3.1 mmol) was added. The mixture was warmed to 25 °C and stirred for 20 h. The reaction mixture was quenched with H<sub>2</sub>O, and the aqueous mixture was extracted with Et<sub>2</sub>O. The organic layer was rinsed with brine and dried with MgSO<sub>4</sub>. Purification by flash chromatography (PE/EA 30/1 to 20/1) afforded 564 mg of **1'** as a pale yellow solid (86% yield). **1'**: pale yellow solid; mp 54–57 °C; <sup>1</sup>H NMR (400 MHz, CDCl<sub>3</sub>)  $\delta$  7.70 (d, *J* = 7.5 Hz, 2H), 7.57 (d, *J* = 7.3 Hz, 2H), 7.35 (t, *J* = 7.3 Hz, 2H), 7.30 (dd, *J* = 10.6, 4.3 Hz, 2H), 5.27 (ddt, *J* = 17.2, 10.1, 7.2 Hz, 1H), 4.88 (dd, *J* = 17.0, 1.1 Hz, 1H), 4.76 (dd, *J* = 10.1, 1.0 Hz, 1H), 2.89 (d, *J* = 7.2 Hz, 2H), 2.57 (t, *J* = 2.3 Hz, 2H), 2.19 (qt, *J* = 7.4, 2.3 Hz, 2H), 1.12 (t, *J* = 7.5 Hz, 3H); <sup>13</sup>C NMR (100 MHz, CDCl<sub>3</sub>)  $\delta$  149.4, 140.4, 133.9, 127.4, 126.9, 123.8, 119.7, 117.6, 84.1, 77.3, 76.5, 52.5, 41.3, 29.6, 14.1, 12.5; FT-IR (neat)  $\nu$  3065, 2931, 2846, 1441, 968 cm<sup>-1</sup>; HRMS (ESI) calcd for C<sub>21</sub>H<sub>21</sub> [*M* + H<sup>+</sup>] 273.1643, found 273.1638.

**General Procedure for the InCl<sub>3</sub>-Catalyzed 1,6-enyne Cycloisomerizations of 1, 1', and 19<sup>7b</sup> in DCE using Chatani's Procedure.**<sup>12</sup> To a mixture of anhydrous DCE (2.5 mL) and InCl<sub>3</sub> (5 or 10 mol %) under argon was added the 1,6-enyne (**1**, **1'** or **19**,<sup>7b</sup> 0.50 mmol). The resulting mixture was stirred at 80 °C for an additional 2 h. The reaction mixture was cooled to room temperature, and the reaction mixture was directly concentrated under vacuum.

The residue was subjected to flash column chromatography on silica gel (eluted with PE/EA 30/1 to 20/1) to give a mixture of diene products and unconverted starting material. The ratios of diene products and unconverted starting material were determined by GC and  $^1\text{H}$  NMR.  $\text{InI}_3$  catalyzed 1,6-enyne (**1**) cycloisomerization in DCE was carried out using a similar procedure (Scheme 3, entry f).

(*E*)-Dimethyl 3-(*But-2-enyl*)cyclopent-3-ene-1,1-dicarboxylate (**2-E**) and (*Z*)-Dimethyl 3-(*But-2-enyl*)cyclopent-3-ene-1,1-dicarboxylate (**2-Z**) Mixture (Scheme 3, Entry a): colorless oil; yield 74%; 2-E: 2-Z = 4:1 determined by  $^1\text{H}$  NMR. NMR of the major *E* isomer (**2-E**):  $^1\text{H}$  NMR (400 MHz,  $\text{CDCl}_3$ )  $\delta$  5.51 – 5.37 (m, 2H), 5.22 (s, 1H), 5.15–5.07 (m, 2-Z), 3.73 (s, 2-Z and 2-E, 8H), 2.99 (s, 2H), 2.92 (s, 2H), 2.78 (d,  $J = 6.6$  Hz, 2-Z), 2.71 (s, 2H), 2.64 (d,  $J = 7.4$  Hz, 2-Z), 1.66 (d,  $J = 5.2$  Hz, 3H), 1.61 (d,  $J = 6.6$  Hz, 2-Z);  $^{13}\text{C}$  NMR (101 MHz,  $\text{CDCl}_3$ )  $\delta$  172.8, 141.0, 127.7, 126.8, 120.7, 59.0, 52.8, 43.1, 40.7, 33.9, 17.9; FT-IR (neat)  $\nu$  1739, 1441, 1259, 1196, 1155  $\text{cm}^{-1}$ ; HRMS (ESI) calcd for  $\text{C}_{13}\text{H}_{18}\text{NaO}_4$  [ $\text{M} + \text{Na}^+$ ] 261.1101, found 261.1097.

(*E*)-3-(*But-2-enyl*)spiro[cyclopent[3]ene-1,9'-fluorene] (**2'-E**) and (*Z*)-3-(*But-2-enyl*)spiro[cyclopent[3]ene-1,9'-fluorene] (**2'-Z**) Mixture (Scheme 4): yield 77%; pale yellow oil; 2'-E:2'-Z = 2.6:1 determined by NMR;  $^1\text{H}$  NMR (400 MHz,  $\text{CDCl}_3$ )  $\delta$  7.67 (d,  $J = 7.3$  Hz, 2H, 2-Z and 2-E), 7.49 (d,  $J = 7.1$  Hz, 2H, 2-Z and 2-E), 7.34–7.23 (m, 4H, 2-Z and 2-E), 5.67–5.43 (m, 3H, 2-Z and 2-E), 2.88–2.95 (26.9 Hz, 2-Z), 2.85 (s, 2H, 2-E), 2.78 (s, 2H, 2-E), 1.69 (d,  $J = 4.5$  Hz, 3H, 2-E), 1.66 (d,  $J = 4.9$  Hz, 2-E);  $^{13}\text{C}$  NMR (101 MHz,  $\text{CDCl}_3$ )  $\delta$  154.3, 154.3, 143.3, 142.7, 139.4, 128.2, 127.6, 127.2, 126.9, 126.6, 125.2, 123.1, 122.4, 119.6, 56.1, 56.0, 48.2, 46.0, 45.9, 34.6, 29.0, 17.8, 12.7; FT-IR (neat)  $\nu$  3304, 3062, 2099, 1643, 1482, 1445  $\text{cm}^{-1}$ ; HRMS (ESI) calcd for  $\text{C}_{21}\text{H}_{21}$  [ $\text{M} + \text{H}^+$ ] 273.1643, found 273.1638.

3-(2-Propenyl)-cyclopentene-1,1-dicarboxylic Acid Diethyl Ester (**20**) and 3-(1-Propenyl)-cyclopentene-1,1-Dicarboxylic Acid Diethyl Ester (**21**) (Scheme 7b). The ratio of **19**, **20**, and **21** determined by GC is ca. 0.23:1.0:1.1, and the ratio determined by  $^1\text{H}$  NMR is about 0.2:1.0:1.1. The combined yield (based on the recovered starting material) of **20** and **21** (1:1.1) is 63%. Pure **20** and **21** can be separated by column chromatography with silica gel impregnated with  $\text{AgNO}_3$ . **20**: colorless oil;  $^1\text{H}$  NMR (400 MHz,  $\text{CDCl}_3$ )  $\delta$  5.60 (t,  $J = 1.8$  Hz, 1H), 4.94 (s, 1H), 4.90 (s, 1H), 3.75 (s, 6H), 3.19 (d,  $J = 1.9$  Hz, 2H), 3.13 (s, 2H), 1.90 (s, 3H);  $^{13}\text{C}$  NMR (100 MHz,  $\text{CDCl}_3$ )  $\delta$  172.6, 141.4, 138.8, 123.7, 113.4, 58.9, 52.9, 41.2, 40.6, 20.4; FT-IR (neat)  $\nu$  2954, 2923, 2853, 1736, 1458, 1437, 1263, 1199, 1166, 1072  $\text{cm}^{-1}$ ; HRMS (ESI) calcd for  $\text{C}_{12}\text{H}_{16}\text{NaO}_4$  [ $\text{M} + \text{Na}^+$ ] 247.0941, found 247.0940. **21**: colorless oil;  $^1\text{H}$  NMR (400 MHz,  $\text{CDCl}_3$ )  $\delta$  6.18 (d,  $J = 15.6$  Hz, 1H), 5.60 (dq,  $J = 15.6$  Hz,  $J = 6.6$  Hz, 1H), 5.41 (s, 1H), 3.74 (s, 6H), 3.07 (s, 2H), 3.10 (d,  $J = 1.4$  Hz, 2H), 1.77 (d,  $J = 6.6$  Hz, 3H);  $^{13}\text{C}$  NMR (100 MHz,  $\text{CDCl}_3$ )  $\delta$  172.5, 139.1, 127.1, 123.5, 58.7, 52.8, 40.6, 39.7, 18.2; FT-IR (neat)  $\nu$  2955, 2916, 2849, 1735, 1435, 1249  $\text{cm}^{-1}$ ; HRMS (ESI) calcd for  $\text{C}_{12}\text{H}_{16}\text{NaO}_4$  [ $\text{M} + \text{Na}^+$ ] 247.0941, found 247.0940.

**150 mol %  $\text{InCl}_3$ -Catalyzed 1,6-enyne (**1**) Cycloisomerization in  $\text{CH}_3\text{CN}$  (Scheme 3, Entry c).** To a mixture of anhydrous  $\text{CH}_3\text{CN}$  (2.5 mL) and  $\text{InCl}_3$  (166 mg, 0.75 mmol) under argon was added **1** (119 mg, 0.50 mmol). The resulting mixture was stirred at 90 °C. After 1 h, the ratio of **1** to (**2-E** + **2-Z**) was found to be about 1.2:1, determined by GC. Some insoluble species were found in the resulting reaction mixture. The reaction mixture was directly concentrated under vacuum. The residue was washed with petroleum ether three times, until GC indicated the disappearance of the starting material in the filtrate. In addition, GC confirmed that **2** was not found in all of the filtrates. The resulting residue was dispersed in  $\text{CH}_3\text{CN}$  (5 mL) as a suspension (it was confirmed by GC that no **1** was in this mixture), which was used for ESI-HRMS analysis. [ $(2+\text{InCl}_2)^+$ ]: HRMS (ESI) calcd for  $\text{C}_{13}\text{H}_{18}\text{Cl}_2\text{InO}_4$  422.96147; found 422.96118; [ $((2)_2+\text{InCl})^+$ ]: HRMS (ESI) calcd for  $\text{C}_{26}\text{H}_{36}\text{Cl}_2\text{InO}_8$  661.08198, found 661.08091.  $\text{InCl}_4^-$ : HRMS-ESI (negative mode) calcd 254.77980, found: 254.77980. 20 mol %  $\text{InCl}_3$  (Scheme 3, entry b) and 400 mol %  $\text{InCl}_3$  (Scheme 3, entry d) catalyzed 1,6-enyne (**1**) cycloisomerizations in  $\text{CH}_3\text{CN}$  used a similar procedure (see the Supporting Information).

**General Procedure for the  $\text{InCl}_3/\text{AgX}$  ( $\text{X} = \text{SbF}_6, \text{BF}_4, \text{OTf}, \text{OCOCF}_3$ )-Catalyzed 1 Cycloisomerizations in DCE (Scheme 3, Entry e).** Anhydrous DCE (5.0 mL) was added to a mixture of  $\text{InCl}_3$  (11 mg, 0.05 mmol) and  $\text{AgX}$  (0.05 mmol) under argon. The mixture was stirred at room temperature for 20 min. To the above mixture was added **1** (119 mg, 0.50 mmol), and the resulting mixture was stirred at 80 °C for an additional 3 h. The reaction mixture was cooled to room temperature and concentrated under vacuum. The residue was subjected to flash column chromatography on silica gel (eluted with PE/EA 30/1 to 20/1) to give a mixture of **1**, **2-E**, and **2-Z**. The ratio of **1**, **2-E**, and **2-Z** was determined by GC (see the Supporting Information for details).

## ■ ASSOCIATED CONTENT

### 📄 Supporting Information

Text, figures, and tables giving  $^1\text{H}$  and  $^{13}\text{C}$  NMR spectra, GC results, more cycloisomerization reactions in  $\text{CH}_3\text{CN}$ , photos of reactions, computational details and further discussions of catalytic species, computed thermodynamic data, and Cartesian coordinates. This material is available free of charge via the Internet at <http://pubs.acs.org>.

## ■ AUTHOR INFORMATION

### Corresponding Author

\*E-mail: yuzx@pku.edu.cn.

### Author Contributions

<sup>†</sup>These authors contributed equally.

### Notes

The authors declare no competing financial interest.

## ■ ACKNOWLEDGMENTS

We thank the Natural Science Foundation of China (20825205-National Science Fund for Distinguished Young Scholars and 21232001) and the National Basic Research Program of China-973 Program (2011CB808603) for financial support. We thank Dr. Jiang Zhou of Peking University for discussions of the ESI-HRMS data.

## ■ REFERENCES

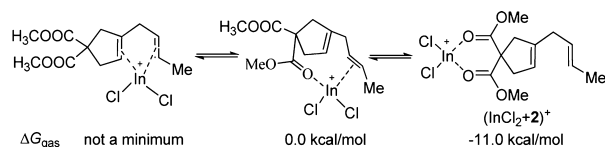
- (1) Crabtree, R. H. *Chem. Rev.* **2011**, *112*, 1536.
- (2) Thome, I.; Nijs, A.; Bolm, C. *Chem. Soc. Rev.* **2012**, *41*, 979.
- (3) For selected recent examples of identifying the catalytically active species by computational studies, see: (a) Robinson, P. S. D.; Khairallah, G. N.; da Silva, G.; Lioe, H.; O'Hair, R. A. J. *Angew. Chem., Int. Ed.* **2012**, *51*, 3812. (b) Corma, A.; Juarez, R.; Boronat, M.; Sanchez, F.; Iglesias, M.; Garcia, H. *Chem. Commun.* **2011**, 47. (c) Proutiere, F.; Aufiero, M.; Schoenebeck, F. *J. Am. Chem. Soc.* **2011**, *134*, 606. (d) Durrant, M. C.; Davies, D. M.; Deary, M. E. *Org. Biomol. Chem.* **2011**, *9*, 7249. (e) Zhang, S.; Ding, Y. *Organometallics* **2011**, *30*, 633. (f) Chow, T. W.-S.; Wong, E. L.-M.; Guo, Z.; Liu, Y.; Huang, J.-S.; Che, C.-M. *J. Am. Chem. Soc.* **2010**, *132*, 13229. (g) Proutiere, F.; Schoenebeck, F. *Angew. Chem., Int. Ed.* **2011**, *50*, 8192. (h) Gruber-Woelfler, H.; Khinast, J. G.; Flock, M.; Fischer, R. C.; Sassmannshausen, J. R.; Stanoeva, T.; Gescheidt, G. *Organometallics* **2009**, *28*, 2546. (i) Zhang, X.; Geng, Z.; Wang, Y.; Li, W.; Wang, Z.; Liu, F. *J. Mol. Struct. (THEOCHEM)* **2009**, *893*, 56. For some examples from our group implicating  $\text{H}_2\text{O}$  as the cocatalyst, see: (j) Liang, Y.; Zhou, H.; Yu, Z.-X. *J. Am. Chem. Soc.* **2009**, *131*, 17783. (k) Liang, Y.; Liu, S.; Xia, Y.; Li, Y.; Yu, Z.-X. *Chem. Eur. J.* **2008**, *14*, 4361. (l) Xia, Y.; Liang, Y.; Chen, Y.; Wang, M.; Jiao, L.; Huang, F.; Liu, S.; Li, Y.; Yu, Z.-X. *J. Am. Chem. Soc.* **2007**, *129*, 3470. (m) Shi, F.-Q.; Li, X.; Xia, Y.; Zhang, L.; Yu, Z.-X. *J. Am. Chem. Soc.* **2007**, *129*, 15503. (n) Liang, Y.; Liu, S.; Yu, Z.-X. *Synlett* **2009**, 905.
- (4) For reviews of indium(III)-catalyzed reactions, see: (a) *Main Group Metals in Organic Synthesis*; Yamamoto, H., Oshima, K., Eds.; Wiley-VCH: Weinheim, Germany, 2004. (b) Yadav, J. S.; Antony, A.;

- George, J.; Subba Reddy, B. V. *Eur. J. Org. Chem.* **2010**, 2010, 591.
- (c) Loh, T. P.; Chua, G. L. *Chem. Commun.* **2006**, 2739. (d) Podlech, J.; Maier, T. C. *Synthesis* **2003**, 633. For selected examples of  $\text{InCl}_3$ -catalyzed reactions of alkynes, see: (e) Xu, Y. L.; Pan, Y. M.; Wu, Q.; Wang, H. S.; Liu, P. Z. *J. Org. Chem.* **2011**, 76, 8472. (f) Montagnac, B.; Vitale, M. R.; Ratovelomanana-Vidal, V.; Michelet, V. *J. Org. Chem.* **2010**, 75, 8322. (g) Montagnac, B.; Vitale, M. R.; Michelet, V.; Ratovelomanana-Vidal, V. *Org. Lett.* **2010**, 12, 2582. (h) Cook, G. R.; Hayashi, R. *Org. Lett.* **2006**, 8, 1045. (i) Hayashi, N.; Shibata, I.; Baba, A. *Org. Lett.* **2005**, 7, 3093. (j) Takami, K.; Yorimitsu, H.; Oshima, K. *Org. Lett.* **2002**, 4, 2993. For a recent example of  $\text{InBr}_3$ -catalyzed reactions of alkynes, see: (k) Surendra, K.; Qiu, W. W.; Corey, E. J. *J. Am. Chem. Soc.* **2011**, 133, 9724.
- (5)  $\text{AlMe}_2\text{Cl}$  was found to use  $\text{AlMe}_2^+$  as the catalyst for Diels–Alder reactions; see: (a) Evans, D. A.; Chapman, K. T.; Bisaha, J. *J. Am. Chem. Soc.* **1988**, 110, 1238. (b) Tietze, L. F.; Schuffenhauer, A.; Schreiner, P. R. *J. Am. Chem. Soc.* **1998**, 120, 7952. (c) Lam, Y.-h.; Cheong, P. H.-Y.; Blasco Mata, J. M.; Stanway, S. J.; Gouverneur, V.; Houk, K. N. *J. Am. Chem. Soc.* **2009**, 131, 1947.
- (6) For recent reviews on the cycloisomerizations of 1,*n*-enynes, see: (a) Lee, S. I.; Chatani, N. *Chem. Commun.* **2009**, 371. (b) Michelet, V.; Toullec, P. Y.; Genét, J.-P. *Angew. Chem., Int. Ed.* **2008**, 47, 4268. (c) Fürstner, A.; Davies, P. W. *Angew. Chem., Int. Ed.* **2007**, 46, 3410. (d) Jiménez-Núñez, E.; Echavarren, A. M. *Chem. Commun.* **2007**, 333. (e) Hashmi, A. S. K. *Chem. Rev.* **2007**, 107, 3180. (f) Marco-Contelles, J.; Soriano, E. *Chem. Eur. J.* **2007**, 13, 1350. (g) Marion, N.; Nolan, S. P. *Angew. Chem., Int. Ed.* **2007**, 46, 2750. (h) Zhang, L.; Sunm, J.; Kozmin, S. A. *Adv. Synth. Catal.* **2006**, 348, 2271. (i) Bruneau, C. *Angew. Chem., Int. Ed.* **2005**, 44, 2328. (j) Añobe, L.; Domínguez, G.; Pérez-Castells, J. *Chem. Eur. J.* **2004**, 10, 4938. (k) Diver, S. T.; Giessert, A. J. *Chem. Rev.* **2004**, 104, 1317. (l) Lloyd-Jones, G. C. *Org. Biomol. Chem.* **2003**, 1, 215. (m) Auber, C.; Buisine, O.; Malacria, M. *Chem. Rev.* **2002**, 102, 813.
- (7) For selected examples of DFT studies of 1,*n*-enyne cycloisomerizations, see: (a) Soriano, E.; Marco-Contelles, J. *Acc. Chem. Res.* **2009**, 42, 1026. (b) Cabello, N.; Jiménez-Núñez, E.; Buñuel, E.; Cárdenas, D. J.; Echavarren, A. M. *Eur. J. Org. Chem.* **2007**, 4217. (c) Nieto-Oberhuber, C.; Muñoz, M. P.; López, S.; Cárdenas, D. J.; Buñuel, E.; Nevado, C.; Echavarren, A. M. *Angew. Chem., Int. Ed.* **2005**, 44, 6146. (d) Soriano, E.; Ballesteros, P.; Marco-Contelles, J. *Organometallics* **2005**, 24, 3172. (e) Soriano, E.; Ballesteros, P.; Marco-Contelles, J. *Organometallics* **2005**, 24, 3182. (f) Soriano, E.; Marco-Contelles, J. *J. Org. Chem.* **2005**, 70, 9345. (g) Nieto-Oberhuber, C.; Muñoz, M. P.; Buñuel, E.; Nevado, C.; Cárdenas, D. J.; Echavarren, A. M. *Angew. Chem., Int. Ed.* **2004**, 43, 2402. (h) Soriano, E.; Ballesteros, P.; Marco-Contelles, J. *J. Org. Chem.* **2004**, 69, 8018. (i) Cabello, N.; Jiménez-Núñez, E.; Buñuel, E.; Cárdenas, D. J.; Echavarren, A. M. *Eur. J. Org. Chem.* **2007**, 4217. (j) Xu, K. L.; Wu, Y.; Xie, D. Q.; Yan, G. S. *Chin. Sci. Bull.* **2004**, 49, 883.
- (8) For selected recent examples of 1,6-enyne cycloisomerizations and applications, see: (a) Camelio, A. M.; Barton, T.; Guo, F.; Shaw, T.; Siegel, D. *Org. Lett.* **2011**, 13, 1517. (b) Jin, T.; Himuro, M.; Yamamoto, Y. *J. Am. Chem. Soc.* **2010**, 132, 5590. (c) Sylvester, K. T.; Chirik, P. J. *J. Am. Chem. Soc.* **2009**, 131, 8772. (d) Chung, C.-P.; Chen, C.-C.; Lin, Y.-C.; Liu, Y.-H.; Wang, Y. *J. Am. Chem. Soc.* **2009**, 131, 18366. (e) Ota, K.; Lee, S. I.; Tang, J.-M.; Takachi, M.; Nakai, H.; Morimoto, T.; Sakurai, H.; Kataoka, K.; Chatani, N. *J. Am. Chem. Soc.* **2009**, 131, 15203.
- (9) Ag (type I): Porcel, S.; Echavarren, A. M. *Angew. Chem., Int. Ed.* **2007**, 46, 2672.
- (10) Au (type I): (a) Nieto-Oberhuber, C.; Muñoz, M. P.; Buñuel, E.; Nevado, C.; Cárdenas, D. J.; Echavarren, A. M. *Angew. Chem., Int. Ed.* **2004**, 43, 2402. (b) Jiménez-Núñez, E.; Claverie, C. K.; Bour, C.; Cárdenas, D. J.; Echavarren, A. *Angew. Chem., Int. Ed.* **2008**, 47, 7892. (c) Bartolomé, C.; Ramiro, Z.; Pérez-Galán, P.; Bour, C.; Raducan, M.; Echavarren, A. M.; Espinet, P. *Inorg. Chem.* **2008**, 47, 11391. (d) Nieto-Oberhuber, C.; Muñoz, M. P.; López, S.; Jiménez-Núñez, E.; Nevado, C.; Herrero-Gómez, E.; Raducan, M.; Echavarren, A. *Chem. Eur. J.* **2006**, 12, 1677.
- (11) Ga (type I): Inoue, H.; Kotsuna, T.; Murai, S.; Chatani, N. *J. Am. Chem. Soc.* **2002**, 124, 10294.
- (12) In (type I and type II): (a) For 1,6-enynes with internal alkynes, type II products were obtained. See: Miyahana, Y.; Chatani, N. *Org. Lett.* **2006**, 8, 2155. (b) For 1,6-enynes with a terminal alkyne, type I products were obtained. See: Nakai, H.; Chatani, N. *Chem. Lett.* **2007**, 36, 1494.
- (13) Ir (types I and II): Inoue, H.; Morimoto, T.; Muto, T.; Murai, S.; Chatani, N. *J. Org. Chem.* **2001**, 66, 4433.
- (14) Pd (type II): (a) Trost, B. M.; Tanoury, G. J. *J. Am. Chem. Soc.* **1988**, 110, 1636. (b) Trost, B. M.; Tour, J. M. *J. Am. Chem. Soc.* **1987**, 109, 4753.
- (15) Pt (type I): (a) Miyahana, Y.; Inoue, H.; Chatani, N. *J. Org. Chem.* **2004**, 69, 8541. Pt (type II): (b) Tsukamoto, I.; Miyano, S.; Inoue, Y.; Oi, S. *Organometallics* **2001**, 20, 3704. Pt (both type I and type II): (c) Furukawa, N.; Sakurai, H.; Murai, S.; Chatani, N. *Organometallics* **1996**, 15, 901. (d) Ferrer, C.; Raducan, M.; Nevado, C.; Claverie, C. K.; Echavarren, A. M. *Tetrahedron* **2007**, 63, 6306. (e) Stelzer, F.; Szillat, H.; Fürstner, A. *J. Am. Chem. Soc.* **2001**, 123, 11863. (f) Fürstner, A.; Szillat, H.; Gabor, B.; Mynott, R. *J. Am. Chem. Soc.* **1998**, 120, 8305. (g) Fürstner, A.; Szillat, H.; Stelzer, F. *J. Am. Chem. Soc.* **2000**, 122, 6785.
- (16) Rh (both type I and type II): (a) Ota, K.; Lee, S. I.; Tang, J.-M.; Takachi, M.; Nakai, H.; Morimoto, T.; Sakurai, H.; Kataoka, K.; Chatani, N. *J. Am. Chem. Soc.* **2001**, 131, 15203. (b) Ota, K.; Chatani, N. *Chem. Commun.* **2008**, 2906.
- (17) Ru: (a) Morimoto, T.; Muto, T.; Murai, S.; Chatani, N. *J. Am. Chem. Soc.* **1994**, 116, 6049. (b) Faller, J. W.; Fontaine, P. P. *J. Organomet. Chem.* **2006**, 691, 1912.
- (18) (a) Nakamura, K.; Osamura, Y. *J. Am. Chem. Soc.* **1993**, 115, 9112. (b) Dean, J. A. *Lange's Handbook of Chemistry*, 15th ed.; McGraw-Hill: Englewood Cliffs, NJ, 1998. (c) In ref 18b, the bond dissociation energy (BDE) of the alkyl C–H bond is 100.1 kcal/mol and that of the allylic C–H bond is 77.4 kcal/mol.
- (19) For two calculation examples using  $\text{InCl}_3$  as the catalytic species, see: (a) Huang, G.; Cheng, B.; Xu, L.; Li, Y.; Xia, Y. *Chem. Eur. J.* **2012**, 18, 5401. (b) Soriano, E.; Marco-Contelles, J. *Organometallics* **2006**, 25, 4542. For a calculation study example of propargyl-allenylindium, see: (c) Miao, W.; Chung, L. W.; Wu, Y.-D.; Chan, T. H. *J. Am. Chem. Soc.* **2004**, 126, 13326.
- (20) Frisch, M. J.; et al. *Gaussian 03, revision C.02*; Gaussian, Inc., Pittsburgh, PA, 2004.
- (21) (a) Becke, A. D. *J. Chem. Phys.* **1993**, 98, 5648. (b) Lee, C.; Yang, W.; Parr, R. G. *Phys. Rev. B.* **1988**, 37, 785.
- (22) (a) Hay, P. J.; Wadt, W. R. *J. Chem. Phys.* **1985**, 82, 299. (b) Dunning, T. H., Jr.; Hay, P. J. In *Modern Theoretical Chemistry*; Schaefer, H. F., III, Ed.; Plenum Press: New York, 1977; pp 1–28.
- (23) Hehre, W. J.; Radom, L.; Schleyer, P. v. R.; Pople, J. A. *Ab Initio Molecular Orbital Theory*; Wiley: New York, 1986.
- (24) (a) Fukui, K. *J. Phys. Chem.* **1970**, 74, 4161. (b) Gonzalez, C.; Schlegel, H. B. *J. Chem. Phys.* **1989**, 90, 2154. (c) Gonzalez, C.; Schlegel, H. B. *J. Phys. Chem.* **1990**, 94, 5523.
- (25) (a) Barone, V.; Cossi, M. *J. Phys. Chem. A* **1998**, 102, 1995. (b) Cossi, M.; Rega, N.; Scalmani, G.; Barone, V. *J. Comput. Chem.* **2003**, 24, 669. (c) Takano, Y.; Houk, K. N. *J. Chem. Theory Comput.* **2005**, 1, 70.
- (26) Reed, A. E.; Curtiss, L. A.; Weinhold, F. *Chem. Rev.* **1988**, 88, 899.
- (27) The  $\text{InCl}_3$ -catalyzed cycloisomerizations of enynes were carried out at 80 °C. The Gibbs free energies of the catalytic cycle at 80 °C can be approximated by using the computed entropies at 298 K.
- (28) Wells, A. F. *Structural Inorganic Chemistry*; Clarendon Press: Oxford, U.K., 1984.
- (29) (a) Cho, J.-S.; Cho, H.-G. *J. Korean Chem. Soc.* **2007**, 51, 287. (b) Cho, J.-S.; Cho, H.-G. *Bull. Korean Chem. Soc.* **2009**, 30, 803. For selected reactions catalyzed by  $\text{In(III)}$  cation species, see: (c) Zhao, J. F.; Tjan, T. B.; Loh, T. P. *Tetrahedron Lett.* **2010**, 51, 5649. (d) Zhao,

J. F.; Tjan, T. B.; Tan, B. H.; Loh, T. P. *Org. Lett.* **2009**, *11*, 5714.  
(e) Zhao, J. F.; Tsui, H. Y.; Wu, P. J.; Loh, T. P. *J. Am. Chem. Soc.* **2008**, *130*, 16492.

(30) Koszinowski, K. *J. Am. Chem. Soc.* **2010**, *132*, 6032.

(31) In the gas phase, we assigned the structure of  $(\text{InCl}_2+2)^+$  as that shown in Figure 1 with both esters coordinated to the In cation due to the coordination of ester being stronger than that of the olefin. In  $\text{CH}_3\text{CN}$  solution, there are many possible complexes among **2**,  $\text{InCl}_2^+$  and solvent, and all these three coordination modes could exist.

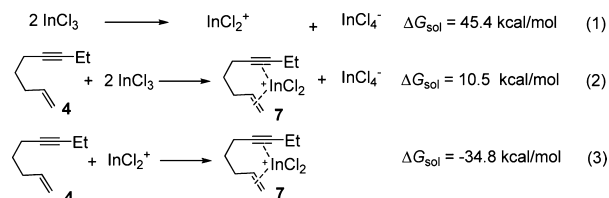


(32) The ratio of **1** to (**2-E** + **2-Z**) was found to be about 1.2:1 in the resulting suspension of reaction under condition c (Scheme 3). The reaction mixture was directly concentrated under vacuum. The residue was washed with petroleum ether three times, until GC indicated the disappearance of the starting material in the filtrate. In addition, GC confirmed that **2** was not found in all filtrates. After the resulting residue was dispersed in  $\text{CH}_3\text{CN}$  (5 mL), GC confirmed that **1** was not present in this suspension. See also the Experimental Section and the Supporting Information for more details.

(33) (a) Einstein, F. W. B.; Tuck, D. G. *Chem. Commun.* **1970**, 1182.  
(b) Habeeb, J. J.; Said, F. F.; Tuck, D. G. *J. Chem. Soc., Dalton Trans.* **1980**, 1161. (c) McGarvey, B. R.; Trudell, C. O.; Tuck, D. G.; Victoriano, L. *Inorg. Chem.* **1980**, *19*, 3432.

(34) Dagorne, S.; Atwood, D. A. *Chem. Rev.* **2008**, *108*, 4037 and references within.

(35) The energies required for the formations of the ions are reasonable considering the following processes. Similar computational results were reported in the generation of cationic  $\text{AlMe}_2^+$  from  $\text{AlMe}_2\text{Cl}$ .<sup>5b</sup>



(36) We also carried out the reaction of **1'** in  $\text{CH}_3\text{CN}$  solution (150 mol %  $\text{InCl}_3$ , 90 °C, 1 h), and we found that this reaction was also stoichiometric, with a conversion of 50%.

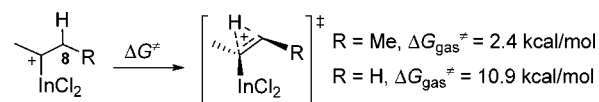
(37) In(III) prefers to be tetracoordinated. Therefore, DCE can stabilize the cyclopropanation and homoallylic cation rearrangement processes (from **9** to **11**) through a chlorine atom coordination to the In center. Without the solvent stabilization, the Gibbs energies of **TS1**, **10**, and **TS2** are 15.5, 4.6, and 11.9 kcal/mol, respectively. Toluene can also play the same role as DCE does; see the discussion of this in the Supporting Information.

(38) (a) The homoallylic cation rearrangement process has also been proposed by Fürstner in their  $\text{PtCl}_2$  catalyzed enyne isomerization.<sup>15fg</sup> Tantillo and co-workers have reported a series of nonclassical carbocation rearrangements; see: (b) Davis, R. L.; Leverett, C. A.; Romo, D.; Tantillo, D. J. *J. Org. Chem.* **2011**, *76*, 7167. (c) Hong, Y. J.; Tantillo, D. J. *J. Am. Chem. Soc.* **2009**, *131*, 7999. (d) Hong, Y. J.; Tantillo, D. J. *Org. Lett.* **2011**, *13*, 1294. (e) Hong, Y. J.; Tantillo, D. J. *J. Am. Chem. Soc.* **2011**, *133*, 18249.

(39) For computational studies of [1,2]-H shifts in carbocation systems, see ref 18a and: Vrček, I. V.; Vrček, V.; Siehl, H.-U. *J. Phys. Chem. A* **2002**, *106*, 1604.

(40) A model study of [1,2]-H shift of cation is presented below. These processes are very facile. The same energy barriers were also found for H-shift processes in ref 39. Furthermore, DFT calculations showed that the Me group is much stronger than H in stabilizing the

cationic transition state, which is consistent with the prediction in part 4 of the text (Scheme 7).

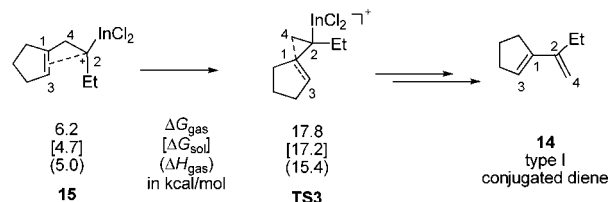


(41) Both **TS<sub>trans-a</sub>** and **TS<sub>cis-a</sub>** lead to trans conjugated dienes. The formation of a cis diene from **15** is not possible due to the coordination of  $\text{InCl}_2^+$  to the C1=C3 bond, causing the Et group to be far away.

(42) (a) Hammond, G. S. *J. Am. Chem. Soc.* **1955**, *77*, 334. (b) Evans, M. G.; Polanyi, M. *Trans. Faraday Soc.* **1938**, *34*, 11.

(43) One reviewer suggested that **21** could be generated by the isomerization of the 1,4-diene **23**. We carefully examined the reaction mixture. Even though we stopped the reaction in 30 min, we did not find any nonconjugated isomer **23**. We can rule out this isomerization pathway on the basis of this experiment. On the other hand, if such double bond isomerization could take place, the reactions shown in Scheme 2 should also give a mixture of conjugated and nonconjugated dienes. This was not observed by Chatani, further proving that there is no isomerization of nonconjugated dienes to conjugated dienes in the cycloisomerization catalyzed by In species.

(44) Via a C1–C4 bond cleavage pathway, **15** can also be converted to the type I product **14**. However, this step via **TS3** requires an activation free energy of 17.8 kcal/mol, significantly higher than the [1,2]-H shifts shown in Figure 5.



(45) Sturla, S. J.; Buchwald, S. L. *Organometallics* **2002**, *21*, 739.

(46) Further study of why ene-terminal-alkyne cycloisomerization catalyzed by  $\text{InCl}_3$  gave a type I diene<sup>12b</sup> will be reported in due course.